Article type: Review

Stimuli-Responsive Surfaces for Switchable Wettability and Adhesion

Chang Li[1,†], Ming Li[2,*†], Zhongshi Ni[3], Qingwen Guan[4], Bamber R. K. Blackman[1], Eduardo Saiz [2]*

[1] Department of Mechanical Engineering, City & Guilds Building, Imperial College London, London SW7 2AZ, United Kingdom.
[2] Centre of Advanced Structural Ceramics, Department of Materials, Imperial College London, London, SW7 2AZ, United Kingdom.
[3] Department of Electrical and Computer Engineering, University of Massachusetts Amherst, Amherst MA 01002, United States of America.
[4] School of Chemistry, University of Glasgow, Glasgow, G12 8QQ, United Kingdom

* Corresponding authors: Chang Li (c.li19@imperial.ac.uk); Ming Li (m.li19@imperial.ac.uk).
† *The two authors contribute equally to this work.*

Abstract: Diverse unique surfaces exist in nature, e.g. lotus leaf, rose petal, and rice leaf. They show similar contact angle but different adhesion properties. According to the different wettability and adhesion charateristics, this review reclassifies different contact states of droplet on surface. Inspired by the biological surfaces, smart artificial surfaces have been developed which respond to external stimuli and consequently switch between different states. Responsive surfaces driven by various stimuli, e.g. stretching, magnetic, photo, electric, temperature, humidity, and pH, are discussed. Studies reporting on either atmospheric or underwater environments are discussed. The application of tailoring surface wettability and adhesion includes microfluidics/droplet manipulation, liquid transport and harvesting, water energy harvesting, and flexible smart device, etc. Particular attention is placed on the horizontal comparison for the smart surface with same stimuli. Finally, the current challenges and future prospects are also identified.

Keywords: bio-inspired, adhesion, wettability, stimuli-response, droplet

1. Introduction

Wettability is an important property of solid surfaces, which has a profound impact on the fields of self-cleaning,[1, 2] micro-fluidic channels,[3] antifouling,[4] fog harvesting,[5] anti-icing,[6] oil/water separation,[7] water energy harvesting[8] and thermal management[9]. In nature, some surfaces show similar contact angles but possess different levels of adhesion. For example, the upper side of a lotus leaf displays superhydrophobic low adhesion surfaces, which are slippery where water liquid could freely move.[10, 11] However, the surfaces of rose petal show high adhesion, on which the water droplets are pinned, though the surface is superhydrophobic.[12] Rice leaf possesses superhydrophobic anisotropic adhesion surfaces, on which droplets are influenced by different forces when moving in different directions.[13] As for some aquatic organisms, for example, filefish,[14] and clam shell[15] have underwater superoleophobic surfaces with low oil adhesion, where oils can easily leave the surface.

Extensive researches have been reported in the literature investigating how diverse micro/nano-structures affect surface wettability, adhesion, and liquid behavior on the surfaces.[16-18] In the past decade, researchers also have fabricated a series of liquid-infused surfaces by injecting lubricant into porous, rough or swellable substrates.[6] To develop multifunctional and intelligent surfaces, there have been many studies concentrating on the constructing of stimuli-responsive materials, where wettability and adhesion can be switched reversibly are focused over the past several years (Figure 1). In this literature review, concepts related to surface wetting for both atmospheric and underwater environment are included. The relationship between wettability, adhesion and liquid behaviour is summarized. As shown in Figure 1, surfaces with diverse wettability and adhesion are reclassified into four contact states. Particular attention is paid to responsive switchable-adhesion surfaces, including

surfaces that respond to the stimuli of stretching, magnetism, light, electricity, and temperature. By reviewing the studies on the responsive surfaces, potential for material design is summarized and proposals for future studies are recommended.

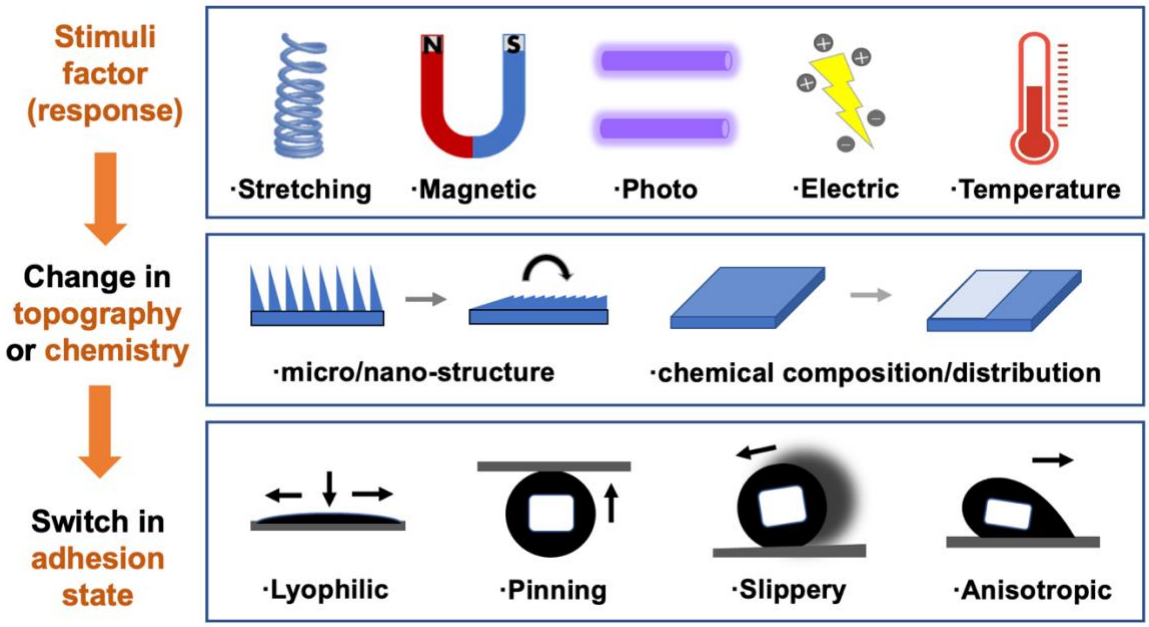

Figure 1. Principle of stimuli-responsive surfaces: stimuli factor (mechanical-stretching, magnetic, photo, electric, temperature, etc) result in change in micro/nano-structure, chemical composition, or chemical distribution; consequently, surface adhesion (contact state) is changed.

2. Theory Basis

2.1 Wettability

Wettability is the property of a surface that describe the degree to which a surface can be wet by a liquid. This property can be quantified by the contact angle (CA), i.e. the value measured through the liquid where an environmental phase-liquid interface meets a solid surface. Generally, a solid surface with a CA<90° is considered to be lyophilic, and a solid surface with a CA>90° is deemed to be lyophobic. For example, when the environment is atmospheric and the liquid is water, a surface with a water contact angle (WCA) >90° is called hydrophobic surface. The critical angle of 90° between lyophilic and lyophobic is derived from the Young's equation.[19] However, Yoon et al.[20] indicated

that the critical angle of hydrophilicity and hydrophobicity was around 65° through the testing of local changes in the chemical potential of water using assistive techniques such as a surface tension meter. Jiang et al.[21] further deduced that the critical limit CA of hydrophilicity and hydrophobicity should be around 62.7°.

In addition, a surface with CA<5° is defined to be superlyophilic, and a solid surface with CA>150° is defined to be superlyophobic. For example, when the environment is underwater and the liquid is an oil, a surface with oil contact angle (OCA) >150° is called an underwater superoleophobic surface.

2.2 Adhesion and contact state

Adhesion, in a broad sense, can refer to the properties of an adhesive joint (solid-adhesive-solid system), or to a combination via Van der Waals force (dry adhesion), surface absorption, and attraction.[22-25] Herein, we focus on any surface-induced obstacles that hinder liquid flow on the surface in any direction or away from the surface, quantified by contact angle hysteresis (CAH), sliding/rolling angle (SA), or relevant force named as adhesive force, retention, resistance, friction.[26, 27]

Surface adhesion is closely related to wettability: on a uniform smooth surface, the larger the contact angle, the smaller the adhesion. However, the situation on practical surfaces is complicated because the micro/nano-structure on the surface may affect the formation of three-phase contact line (TPCL). A typical example is rose petal, on which the water droplets are pinned, though the surface is superhydrophobic.[12] In fact, both adhesion and wettability of the surface are firmly associated with surface chemical composition, chemical distribution, and topography. By changing these factors, surface adhesion to liquid can be adjusted to control contact situation between liquid and surface.

Based on the difference in wettability and adhesion, here we divide the liquid behaviour on surface into four typical contact states (Table 1, Figure 1).

Table 1. Different surface contact states and the corresponding liquid behaviour

Contact State	Description of the State	Liquid Behaviour on Surface
Lyophilic	Ultra high adhesion	Droplet can wet the surface or even spread flat.
Pinning (rose petal)	Lyophobic but high adhesion	Droplet turns spherical, and stays still on the surface.
Slippery (lotus leaf)	Lyophobic and low adhesion	Droplet turns spherical, and can easily slide/roll off.
Anisotropic (rice leaf)	High retention for one direction and low retention for another	Droplet tends to move directionally.

3. Responsive surfaces

Artificial smart surfaces, which are designed to possess stimuli-responsive wettability and adhesion, can transfer from one state to another are introduced in this section.

3.1 Stretching-responsive surfaces

Mechanical stretching (strain) can alter the bulk and surface geometry of a soft material, consequently enabling the reversible control of surface adhesion. Simply enlarging or compressing the material will not change the surface tension or chemical composition.[28] However, the surface roughness will be notably changed, which would influence the CAH and other adhesion properties of the surface, resulting in different liquid behaviour (Table 2).[29-31]

Table 2. Comparison of typical stretching-responsive surfaces

Structural Feature	**Advantages**	**Ref.**
Responsive SLIPS	Can realise SA change without CA change, switching between pinning and slippery state	[32]
Micropillar arrays structured soft substrate	Can realise CAH change and droplet deformation	[33]
Asymmetric-stretching on soft materials	Switching between anisotropic and pinning state, can realise unidirectional droplet motion	[34]
Soft striped-microgroove surface	Can realise SA change without CA change, switching between pinning and slippery state, can realise unidirectional droplet motion	[35]

The strain response can be utilised on a slippery lubricant-infused porous surface (SLIPS),[36-39] where either pinning or the slippery state can be obtained respectively. Yao et al. combined a porous Teflon nanofiber network with an elastic polydimethylsiloxane (PDMS) membrane to obtain a stretchable substrate.[32] Perfluoropolyether was then infused into the porous substrate as the lubricant so that the stretchable SLIPS was achieved. When the SLIPS was compressed, the diminished nanopores contributed to lubricant release. The lubricating layer (Figure 2a, b) gave rise to a much lower adhesion surface (slippery state). By elongating the SLIPS via external mechanical tension, the nanopores were enlarged. Lubricant flowed to the nanopores, resulting in a higher adhesion surface causing water pinning (Figure 2b, 2c). As shown in Figure 2d, the SA of different liquid on such a mechanical stretching response surface could range from 5° to 25°. This kind of material will have an application prospect in the field of droplet manipulation.

Coux et al.[33] studied the stretching response on a micropillar arrays structured soft PDMS substrate. They found that surface wettability and CAH changed as a function of surface dilation ($\sum$). When the substrate was elongated, the shape of the micropillars were slightly changed but the intensity of micropillars was sharply reduced (Figure 2e). As shown in Figure 2f, 2g, such an intensity reduction finally caused a lower contact angle and a higher surface adhesion. Su et al.[40] fabricated a Janus PDMS and found that the Laplace driving force and wettability gradient driving force for water movement could both be controlled through stretching or compressing the substrate. It was suggested that such material will have application not only in fog harvesting, but also on dynamic fog-flux regulators.

The strain response can also be designed on soft anisotropic materials. Zhang et al.[34] studied the asymmetric-stretching response on a stripe-microgroove structured organogel composed of poly(butyl methacrylatecolauryl methacrylate) and silicone oil. Unidirectional droplet motion was achieved via asymmetrically stretching the soft organogel. As shown in Figure 2h, when the organogel was elongated vertical to the groove direction from one side, the water droplet can easily move (water slide angle WSA≤10°) from the elongated side to non-elongated side. By contrast, water droplet was pinned when it comes to moving against (Figure 2i). They suggested that the switch in adhesion was caused by the asymmetric-stretching induced fan-shaped grooves, which act as a physical barrier that guides the droplet movement. The roughness variation had only a minor effect. Wang et al.[35] studied the bending and stretching response on a soft skinlike (striped microgroove) PDMS. When the strain was applied perpendicular to the stripe direction, WCA remained over 140° but WSA ranged from 3° to the pinning state, as shown in Figure 2j. The surface was reversely switched from the lotus leaf state

to the rose petal state. Taking advantage of the soft materials, the stretching-responsive surfaces can be further designed as wearable device, or other flexible smart device.

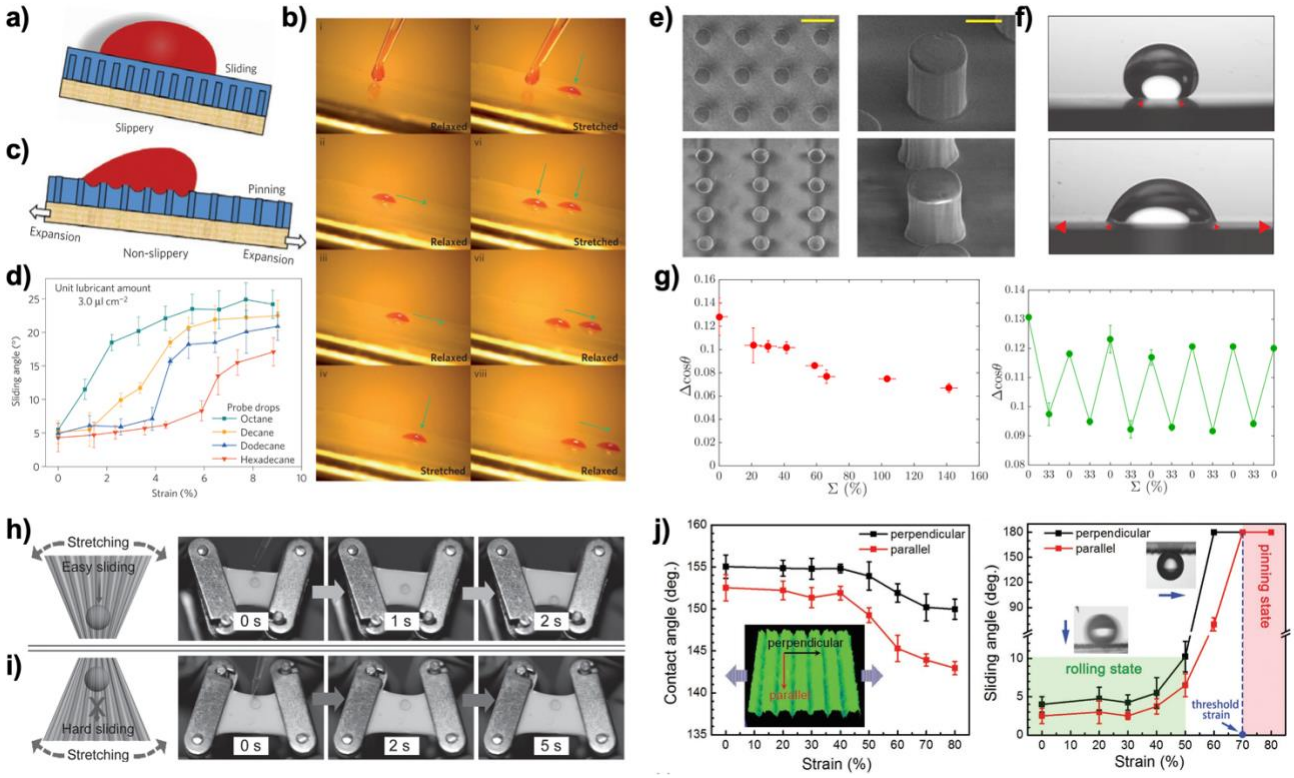

Figure 2. Mechanical stretching response on smart materials (in air). a-d) Stretching response on a SLIPS, from slippery to non-slippery. Reproduced with permission.[32] Copyright 2013, Springer Nature. e-g) Stretching response on a micropillar array surface, switch in CA and CAH. Reproduced with permission.[33] Copyright 2017, American Institute of Physics. h-i) Asymmetric-stretching response on a stripe-microgroove surface, unidirectional adhesion. Reproduced with permission.[34] Copyright 2014, Wiley-VCH. j) Stretching response on a soft skinlike surface; switch between lotus leaf state and rose petal state. Reproduced with permission.[35] Copyright 2018, Wiley-VCH.

3.2 Magnetic-responsive surfaces

Atmospheric environment

A magnetic substance can be incorporated into the substrate during manufacture to obtain a magnetic responsive surface. The surface roughness and/or microstructure could then become controllable via

an external magnetic field, so as to adjusting the wettability and adhesion (Table 3).[41-43] By controlling these factors, droplet manipulation, water collection, or liquid transport can be realised. Also, these controllable surface would be useful for designing or manufacturing microfluidic devices.

Table 3. Comparison of typical magnetic-responsive surfaces

Structural Feature	**Control Avenue**	**Advantages**	**Ref.**
Magnetic fluid in nanoarray (in air)	Adjusting the intensity of magnetic field	can control CA, realising unidirectional droplet motion, antigravity motion, and motion at different speeds	[44]
Flexible magnetized conical array (in air)	Adjusting the direction of magnetic field	can realise change in SA and retention force, can realise and control droplet directional bouncing	[45, 46]
FLIPS (in air)	Applying or removing magnetic field	can realise SA change to control droplet displacement, switching between pinning and slippery state	[47, 48]
Two uniform-nanorods structured substrates (under water)	Applying periodic magnetic field	can realise reversibly oil droplet transferring between substrates	[49]

Generally, to make an material magnetic-responsive, magnetic substance need to be added. Tian et al.[44] added an Fe_3O_4 magnetic fluid into an ZnO nanoarray to obtain a magnetic responsive surface. As shown in Figure 3a, by adjusting the intensity of the external magnetic field, the surface could be switched between having a smooth and rough microstructure, showing different contact angle and adhesion. By further varying the magnetic field, unidirectional droplet motion, antigravity motion, and motion at different speeds were easily realised.

A conical array structured surface can be magnetized to become a smart material. Peng et al.[50] added Co magnetic particles to PDMS during the curing process of the soft lithography to obtain a magnetic-responsive microcone-array structured surface. As shown in Figure 3b, the conical arrays were vertical when the external magnet was placed directly above the surface. Moving the magnet to the right or

left, the conical arrays were attracted to the magnet. Also, by applying the magnetism as a cyclic function periodic vibration of the microcone arrays was achieved, improving fog capturing performance due to the optimized contact area with moisture and the Laplace driving force. If required, the permanent bending of the micro arrays could also be realised using this method. Li et al.[45] made use of the Co magnetic response during the preparation and achieved arrays which displayed diverse permanent obliquity. The WSA ranged from over 60° to below 5° and the retention force ranged from over 80 μN to below 20 μN on account of the different obliquity. They also found that a water droplet showed a directional bouncing trend on the bent arrays. The horizontal displacement sharply increased, and the bounce height slightly decreased with the arrays bending from vertical to 45° obliquity. Lin et al.[46] realised diverse permanent bending by means of magnetization and indicated that a very slight vertical vibration (e.g. wind, sound) would cause droplet movement towards the bending direction.

A magnetic response could also be imparted to SILPS by using magnetic substances as lubricants. Wang et al.[47] employed a ferrofluid when preparing SILPS (namely FLIPS). When no magnetic field was applied, magnetic nanoparticles were disturbed randomly, showing a relatively smooth surface (Figure 3c). However, external magnetic field gradient could redisturb the magnetic nanoparticle in the ferrofluid. As shown in Figure 3c, 3d, the ferrofluid showed a multiscale hierarchical topographical shape. Consequently, the adhesion force (Figure 3e) against water movement was controlled accurately and reversibly. For example, Figure 3f shows the totally different adhesion properties to droplets when diluted ferrofluids are employed.

Huang et al.[48] combined the concept of FILPS with the magnetic responsive microcone-array (Figure 3g). As shown in Figure 3h, the micro-array could be deformed between the states of being flat (0°) and perpendicular (90°) by application of the external magnetic field. The droplet bouncing

and sliding test showed that, when the micro-array was perpendicular to the surface, the droplet was pinned to the surface (Figure 3i), indicating high adhesion. Adjusting the magnetic field to make the micro-array lie down, the droplet came into nearly full contact with the slippery lubricant, releasing the droplet (Figure 3j). Li et al.[51] used a similar strategy and produced a PDMS@Fe_3O_4 coated fabric. They found that different Fe_3O_4 concentrations could lead to different values of WCA. By adjusting the magnetic response, the surface wettability and adhesion could be reversibly transformed.

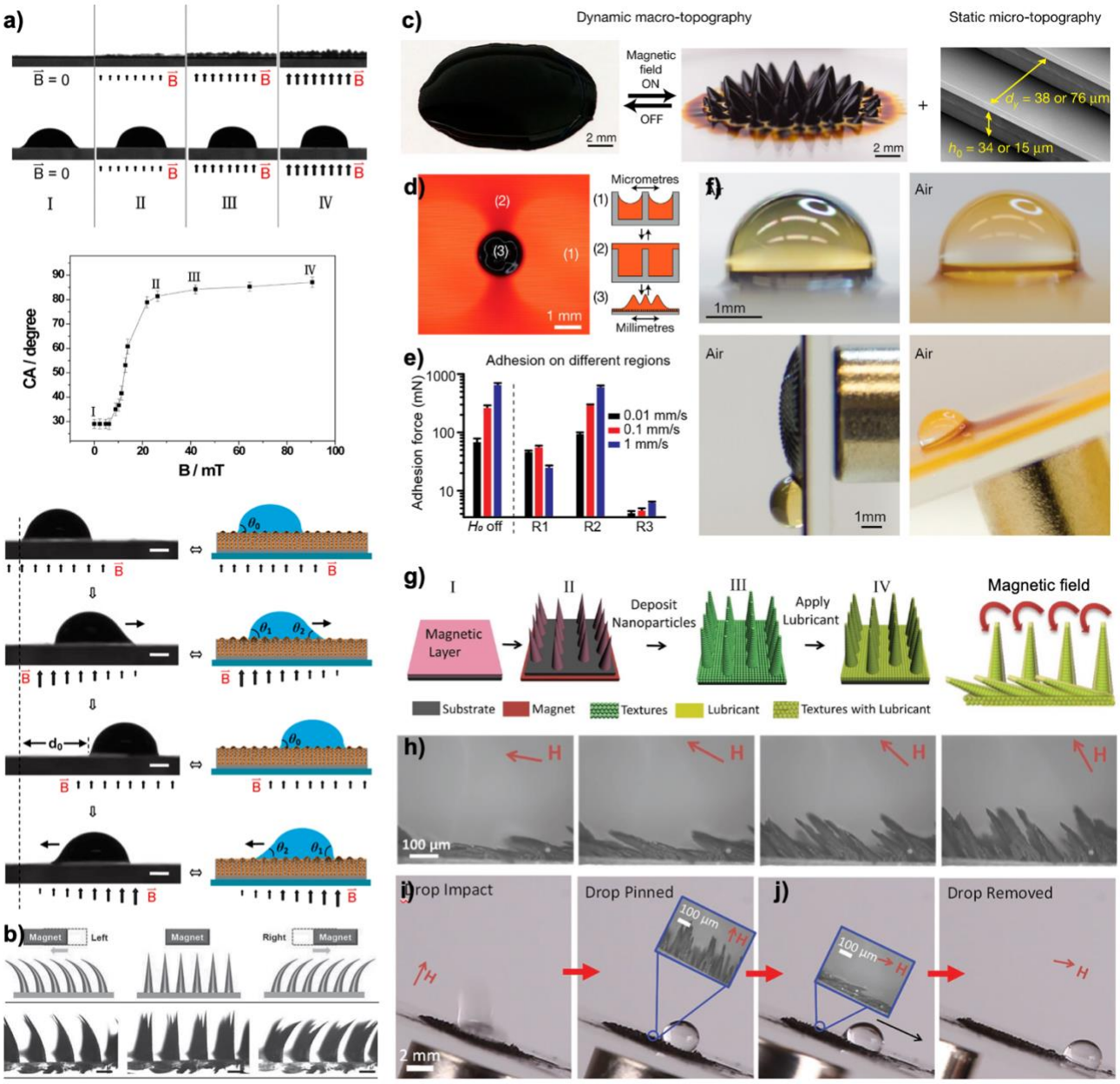

Figure 3. Magnetic response on smart materials (in air). a) Response on magnetic fluid/ZnO nanoarray composite interface, switch in surface roughness, CA and adhesion; Reproduced with permission.[44] Copyright 2016, American Chemical Society. b) Response on conical array structured surface, switch in microstructure; Reproduced with permission.[50] Copyright 2015, Wiley-VCH. c-f) response on FILPS, switch in macro/micro-structure, adhesion force, and adhesion performance; Reproduced with permission.[47] Copyright 2018, Springer Nature. g-j) Response on lubricant-containing conical array structured surface, switch between pinning state and slippery state. Reproduced with permission.[48] Copyright 2017, Wiley-VCH.

Underwater environment

Recently, Feng et al.[49] demonstrated a method for driving oil-based magnetic fluids using an external magnetic field. They first used a low-temperature hydrothermal method to grow a uniform array of ZnO nanorods on a glass substrate. This ZnO surface showed superoleophobicity under water after UV treatment (OCA = 156°, oil slide angle OSA<5°, Figure 4a). Then, they used two ZnO surfaces with the above properties to move oil droplets in water. As shown in Figure 4b, one substrate (top) was suspended above the other substrate (bottom), making them opposite and leave proper space in the middle. The magnetic oil droplets (i.e., silicone oil containing Fe_3O_4 nanoparticles) were injected onto the lower substrate. By applying a periodic external magnetic field to the system as a driving force, they found that the oil droplets were able to quickly respond to the stimulation of the external magnetic field, reversibly transferring between the two substrates. During the entire oil droplet movement, there was no adhesion of magnetic oil droplets to the substrate due to the low oil adhesion of the ZnO nanorod array to the magnetic oil. Conversely, when two smooth ZnO substrates were used for the same transmission experiment, a noticeable delay in the movement of the oil droplets was observed. These findings might be useful for oil/water separation and underwater anti-fouling devices.

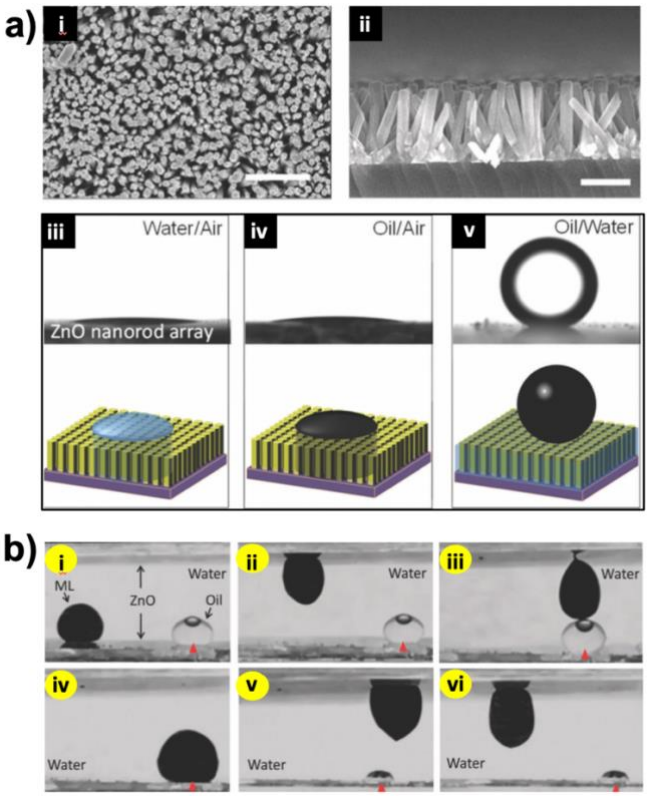

Figure 4. Magnetic response on smart surfaces (under water). a) Morphology and wettability characterization of the aligned ZnO nanorod arrays. b) The manipulation and transfer of an underwater oil droplet by a magnetic fluid droplet on the aligned ZnO nanorod arrays. Reproduced with permission.[49] Copyright 2016, The Royal Society.

3.3 Temperature-responsive surfaces

Atmospheric environment

Increasing the temperature may give rise to the partial melting of a solid which then introduces a liquid layer between the solid surface and the droplet so that the surface adhesion switches.[15, 52] Yao et al.[53] realised a temperature-responsive surface adhesion on a n-paraffin-swollen organogel surface. At room temperature, the rough surface was in a high adhesion state with high adhesive force (over 200 μN) and water droplet pinning. When the temperature was raised to 58-60 °C, the n-paraffin partly transformed to the liquid phase, making the surface slippery. The surface transformed into a low adhesion state with a low adhesive force (around 40 μN) and a WSA of approximately 6°. Decreasing the tempertaure could then solidify the n-paraffin to realise the reversible switch of surface adhesion.

Increasing the temperature to the glass transition temperature of a flexible polymer can activate molecular chain mobility and alter the elasticity of the polymer.[54-58] Employing such a flexible polymer with shape memory can achieve the reversible control of surface microstructure, which further controls the adhesion.[54, 59, 60] For instance, Cheng et al.[61] fabricated a microarray structured surface using a shape memory polymer. As shown in Figure 5a, the microarray was uniform and vertical, and the surface showed a superhydrophobic (WCA=151°±1.5°) isotropic adhesion (WSA=24°±1.2°) similar to the lotus leaf. When the surface was thermally-pressed at a temperature slightly above the glass transition temperature, the pressed pillars laid down, turning into a microgroove-like structure. The surface showed an anisotropic adhesion property similar to the rice leaf. The WSA in the A direction was 20°±1.3°, and the WSA in the B direction was 29°±1.5° (Figure 5a). When the surface was reheated under the same temperature, the pillar would stand vertically, thus the reversible switch between superhydrophobic isotropic adhesion and anisotropic adhesion is achieved (Figure 5b). They also realised the lie-down of appointed pillars in the surface, where the water moved controllably. Such smart surfaces may potentially be applicated in bioseparation or microfluidic devices.

Increasing the temperature to the lower critical solution temperature (LCST) for some block copolymers can give rise to a polymeric transformation from the extended state to the collapsed state.[62-64] N-isopropylacrylamide (PNIPAAm) based polymer is a good example, where the surface roughness may change with the increasing temperature. More significantly, PNIPAAm-based material will transform the hydrogen bonding between intra- and inter-molecular under different temperature,[65, 66] causing a notable change in wettability and adhesion. Hou et al.[67] found that the values of WCA and CAH on PMMA-b-PNIPAAm (PMMA: poly(methyl methacrylate)) were

51.64° and 43 ° at 20 °C, respectively. When the temperature was raised to 45°, the surface morphology of the polymer changed as the polymeric state transformed. The values of WCA and CAH increased to 107.09° and 60° repectively, indicating a correlation between the temperature and the surface wetting property. Li et al.[68] fabricated a peristome-beak surface inspired by the nepenthes and shorebird using PNIPAAm based microgel. Water showed different spreading behavior on the surface due to the temperature responsive switch in adhesion force value and direction. As shown in Figure 5c, when the temperature was 20 °C, the droplet unidirectionally flowed along the striped microgrooves. As shown in Figure 5d, when the substrate was heated to 40 °C, the droplet spread bidirectionally across the microgrooves, and was pinned at overhangs. Such designs may have application in not only microfluidic but also heat-transfer system.

Temperature changes may also have complex effects upon the results of wettability and adhesion tests, especially in an atmospheric environment (Table 4). Noteworthy is the fact that on an overheated surface, water droplet may be levitated by its self-generated vapor. This phenomenon is called Leidenfrost effect.[69] Zhong et al.[70] reviewed how surface topography and wettability affected the Leidenfrost effect, with a view to droplet geometry and dynamic. Recently, Graeber et al.[71] observed a more complex motion of droplet on overheated surface termed Leidenfrost droplet trampolining. However, heating a substrate sometimes causes notable variation in environmental humidity and the liquid physicochemical properties.[72-75] These effects should not be ignored, and therefore should be investigated in future research. In addition, the temperature related response could also be designed as an electricthermal response and a photo-thermal response. These are discussed in the following two sub-sections.

Table 4. Comparison of typical temperature-responsive surfaces

Control avenue	Applicable materials	Advantages	Ref.
Partial melting of a solid surface introducing a liquid layer/solidifing the layer (in air)	Organogel, e.g. n-paraffin-swollen organogel	can realise change in SA and adhesive force	[15, 52, 53]
Increasing/decreasing the temperature to the glass transition temperature (in air)	Thermoelastic polymer (microstructured)	switching between isotropic and anisotropic state, can realise droplet directional motion	[54, 59-61]
Increasing/decrease the temperature to the LCST (either in air or under water)	Block polymers, e.g. PNIPAAm based polymer	can realise change in CA/adhesion, can control the direction of droplet motion	[67, 68, 76-78]
Leidenfrost effect (in air)	Heat-resisting materials	can control droplet geometry and dynamic	[70, 71]

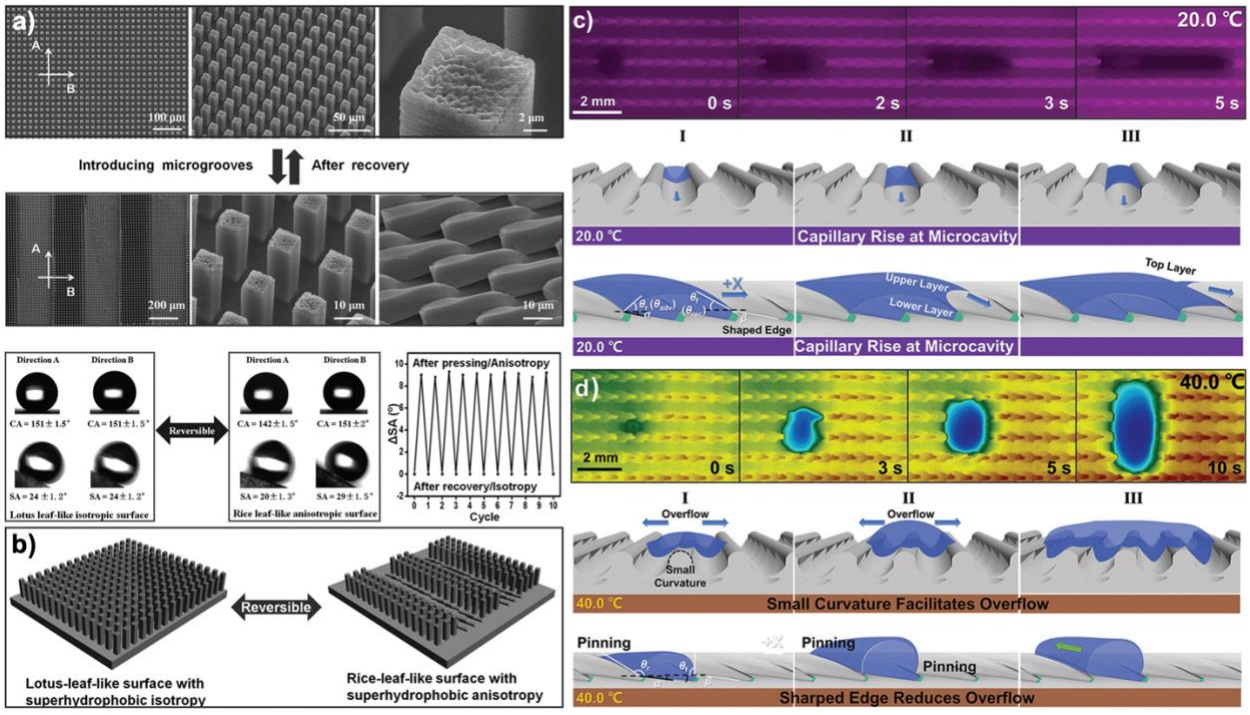

Figure 5. Temperature/thermal response on smart surfaces (in air). a-b) On a micropillar array structured shape memory polymer, adhesion switch between isotropy to anisotropy; Reproduced with permission.[61] Copyright 2018, Wiley-VCH. c-d) On a bio-inspired peristome-beak structured PINPAAM based microgel, switch in adhesion force value and direction giving rise to change in water spreading behaviour. Reproduced with permission.[68] Copyright 2018, Wiley-VCH.

Underwater environment

In addition to the researches carried out in air, PNIPAAm based materials are also employed for underwater studies. Heating the material around LCST, the adhesion of oil droplets to the surface will be changed. Oil droplet will then show different behaviours on the surface. Therefore, underwater oil droplet manipulation are realised, which can be further applied for oil/water separation, underwater anti-fouling, etc.

Chen et al.[78] prepared a thermally responsive PNIPAAm hydrogel. The surface wettability and the adhesion to oil droplets were related to the temperature of the surrounding aqueous solution. When the temperature of the solution was lower than the LCST (32 °C) of PNIPAAm, the surface showed underwater superoleophobicity and low oil adhesion, i.e. the underwater OCA was 151.7°±1.6°, and oil-adhesion force was 5.8 μN. When the temperature of the solution was raised to above the LCST, the surface showed weak oleophobicity and high oil adhesion. At this time, the underwater OCA of the hydrogel decreased to 127.0°±4.6°, and the adhesion increased to 23.1 μN. They also found that the two different states could be switched reversibly multiple times. The PNIPAAm hydrogel displayed this performance due to the large number of hydrophobic groups (–$CH(CH_3)_2$) and hydrophilic groups (–CONH–) contained in its network. At room temperature (<LCST), the N–H/C=O groups on the branch of PNIPAAm formed an intermolecular hydrogen bond with water molecules in the solution, which made the gel hydrate and swell. The trapped water layer further realised the superoleophobicity and low oil adhesion. However, when the solution temperature was rasied above the LCST, the N-H/C=O groups in the hydrogel formed intramolecular hydrogen bonds with the molecules on the adjacent branches. This formation made the hydrogel dehydrate and collapse, losing the repulsion to oil droplets, finally reducing the oleophobicity and enhancing the adhesion to oil.

Liu et al.[77] reported the silicon nanowire array-modified heptafluorodecyltrimethoxysilane (HFMS) and heat-sensitive PNIPAAm (Figure 6a). The switch between superoleophilic state and superoleophobic state of the surface was achieved by adjusting the water temperature. As shown in Figure 6b, the surface was superoleophobic in water at 20 °C, and the underwater OCA (1,2-dichloroethane, 2 μL) was 157°. However, when the ambient temperature increased, it became superoleophilic, and the underwater OCA was only 3° at 60 °C. They also found that the transition between the underwater superoleophobicity (20 °C) and the underwater superoleophilicity (60 °C) was reproducible (Figure 6c). The switchable adhesion is mainly derived from the grafted PNIPAAm chain which could cover or expose oleophilic HFMS components through the change of thermally responsive molecular structure. At room temperature, the PNIPAAm chain preferentially bonded with water molecules in solution to form intermolecular hydrogen bonds. The hydrated PNIPAAm chain tended to extend further outward, so that the oleophilic HFMS chain was covered and hidden, causing underwater superoleophobicity. As the temperature was increased to 60 °C, the PNIPAAm chain mainly generated intramolecular hydrogen bonds among its branches, which caused the dehydration shrinkage of the grafted PNIPAAm chain, exposing the oleophilic HFMS chain to form an underwater superoleophilic surface (Figure 6c, 6d).

Inspired by the predation mechanism of sundews in nature, Ma et al.[76] constructed a new PNIPAAm based hydrogel actuator with high mechanical strength and asymmetric structure (Figure 6e). The hydrogel actuator could not only respond to environmental temperature changes (LCST of PNIPAAm) and achieve reversible switching of surface adhesion (Figure 6f), but also could realise fast solvent exchange between ethanol and water. In addition, the actuator was able to perform reversible responsive bending, accompanied by an actuating force (≈21mN), which enabled the actuator to

reversibly capture and release under-water oil droplets (Figure 6g).

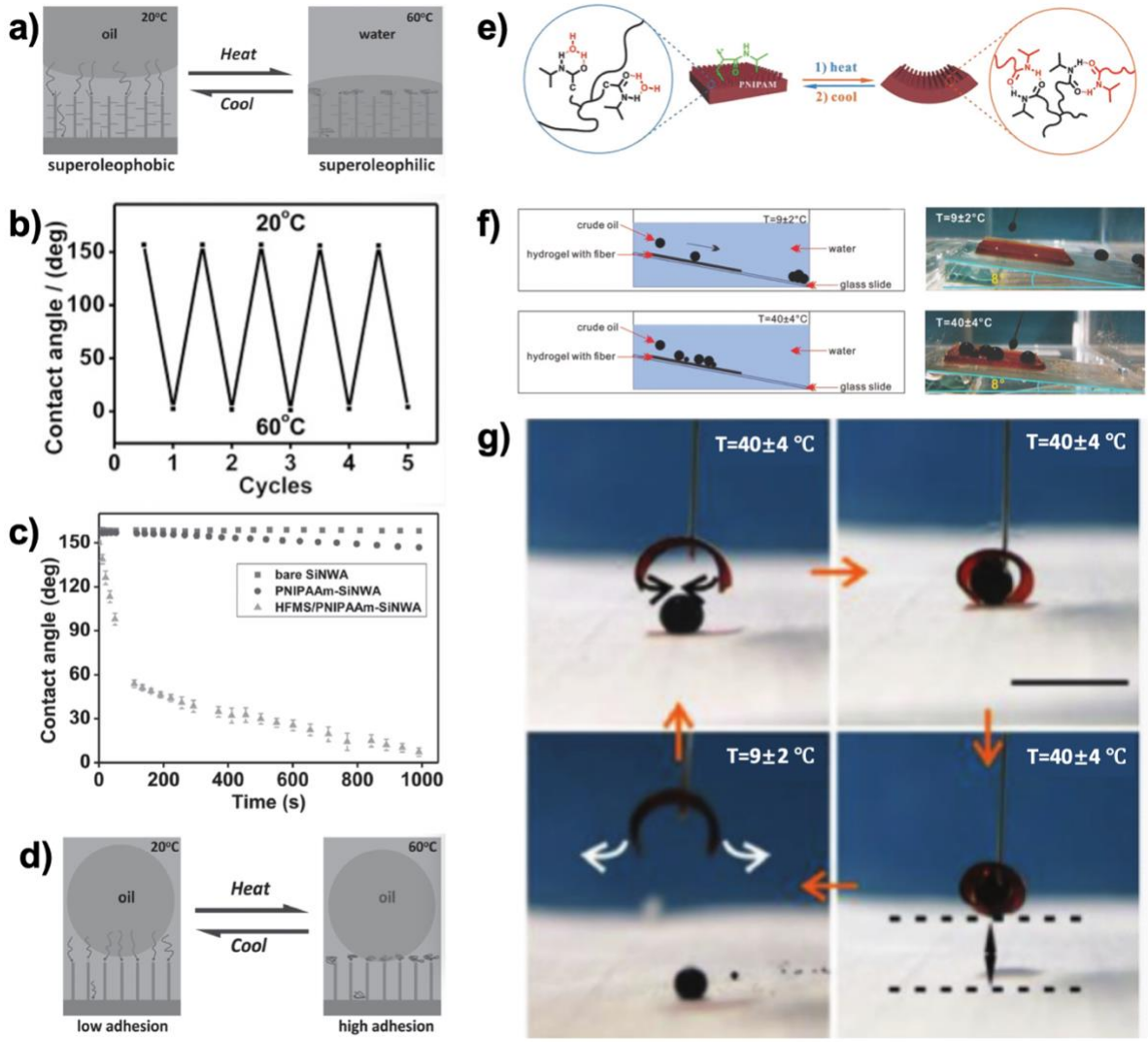

Figure 6. Temperature response on smart surfaces (under water). a-d) PNIPAAm-HFMS surface: Reproduced with permission.[77] Copyright 2015, Wiley-VCH. a, b) Underwater temperature-responsive PNIPAAm-HFMS surface, and the changes of underwater contact angles are repeatable. c) Real-time underwater contact angles of DCE droplets with different chemical compositions at 60 °C. d) Underwater temperature-responsive switch between low and high adhesion on PNIPAAm-SiNWA. e-g) PNIPAAm hydrogel: Reproduced with permission.[76] Copyright 2019, Wiley-VCH. e) The conformational change mechanism of the PNIPAAm polymer chains with water molecules responsible for the thermo-responsive curving Behaviour of the hydrogel film. f) Schematic diagram and snapshot showing dynamic sliding of oil drop on fibrillar side and nonstructured side of the hydrogel film at high (40 °C) and low (9 °C) temperature condition. g) Reversibly capturing and releasing the oil droplet by thermo-responsive bending of the hydrogel film underwater.

3.4 Electric-responsive surfaces

Atmospheric environment

An electric field can affect surface wettability, adhesion, and liquid behavior in various ways (Table 5). For example, the WCA can be reduced by applying an electric field between a conducting droplet and a counter electrode underneath the droplet, which is an electrowetting course without changing the surface structure.[28, 79] Previous studies indicated that by changing the applied voltage during electrowetting, the CA could be accurately adjusted; the adhesion and liquid behavior could also be controlled using this strategy.[80]

Table 5. Comparison of typical electric-responsive surfaces (in air and underwater)

Control avenue	**Materials**	**Surface topography**	**Characteristic after electric field applied**	**Advantages**	**Ref.**
Electrowetting effect	Conductor	Not change	CA reduces	can accurately adjust CA and control droplet motion	[28, 79, 80]
	SLIPS using conducting substrates	Not change	Pinning state (effectiveness of lubricants reduces)	can realise the switch between pinning state and slippery state	[81, 82]
	Conductive polypyrrole (PPy) film	Not change	Underwater OCA increases	can control the movement of underwater oil droplets or bubbles	[83]
New electro-dewetting mechanism	Super-hydrophilic conductor	Not change	CA increases	can realise droplet directional moving, merging, and splitting	[84]
Effect of electric potential on dodecyl chains	Dodecyl chains based materials	Change	Superhydrophilic state (electric potential rotated hydrophobic dodecyl)	can realise the switch between superhydrophilic state and slippery state	[85]
Electric-thermal expansion effect	SLIPS using flexiable substrates	Change	Pinning state (lubricants penetrate into expanded porous)	can further realise complex droplet behavior, e.g. oscillation, jetting	[86, 87]
Electrochemical reaction	Binary composite metal surface	Change	Underwater OCA reduces	can control the oil spreading on surface	[88]
Electrochemical oxidation	Conductive polymer PANI	Not change	Underwater OCA reduces	can control the oil adhesion on surface	[89]

Guo et al.[81] applied a bar electrode above a SLIPS where the upper side of the droplet was in contact with the electrode. When there was no applied voltage, the surface was in the slippery state due to the lubricant (Figure 7a). When the voltage was applied, the microstructure of the surface was not changed but the droplet remained on the surface (Figure 7b). They suggested that the switch in adhesion was caused by the electrostatic attraction between the SLIPS and the liquid, which reduced the effectiveness of the lubricant. Wang et al.[82] further found that the responsive voltage could be reduced by employing lubricants with a lower viscosity during SLIPS fabrication.

Li et al.[90] controlled liquid motion via an electric corona discharge on a polyethylene terephthalate (PET) film coated Cu electrode. They drilled a hole into the PET where the conductive substrate was exposed to the direct current (DC) power needle. A silicone oil droplet was released onto the PET surface near the hole and it showed a flat-ellipsoid shape. When the DC power was applied, the droplet immediately jumped into a spherical shape, moving horizontally away from the hole, as shown in Figure 7c. The displacement of the oil droplet was affected by the distance between the droplet and the conductive hole. Furthermore, Plog et al.[91] studied the electric responsive movement of ink droplets which have diverse chemical composition and droplet size on the Cu electrode-embedded substrate (Figure 7d). They realised the accurate motion control of commercially pure-liquid, carbon fibre suspension, and polymer solution ink droplet in 200 μm-3mm diameters by adjusting the applied voltage.

Recently, Li et al.[84] developed a novel mechanism termed electro-dewetting. They used employed a bare silicon wafer as a highly hydrophilic substrate and an ionic surfactant as a droplet. In stark contrast to conventional electrowetting, the contact angle did not decrease but rather increased when the voltage and current were applied. It was explained that the interaction between the droplet and the

conductive substrate was not directly controlled by the voltage. As shown in Figure 7e, the electro-dewetting probably resulted from the electric field-induced adhesive interaction change of the ionic surfactants to the hydrophilic substrate. By changing the direction of the electric field, the ionic surfactant molecules migrated towards or away from the hydrophilic substrate, realizing electro-dewetting and rewetting. Under this novel mechanism of electric-field responsive change of adhesion, droplet directional moving, merging, and splitting were realsied, as shown in Figure 7f. This finding open the door for board application related to microfluidics.

An electric field can also adjust the surface wettability and adhesion by switching the structure in some smart materials.[92, 93] Liu et al.[85] utilized the effect of electrical potential on the dodecyl chains to fabricate an electric responsive porous membrane. The electric potential rotated the hydrophobic dodecyl chains to conceal the pores. This transformation enables the switch in surface wettability from superhydrophobic low adhesion (WCA around 152°, WSA around 4°) to superhydrophilic state (WCA near 0°). They also found that an organic reagent rinsing process could re-rotate the hydrophobic dodecyl chains to recover the superhydrophobicity, realizing the reversible switch in surface property (Figure 7g). They found that such a surface could act as a smart liquid gate for sensor, efficient water/oil separation, and controllable liquid transfer. An electric response can also be obtained by electric-thermal expansion. For example, Wang et al.[87] prepared a SILPS using shape-memory graphene (GO) film as the substrate. The GO could be compressed to a desired initial length. Then, a constant DC voltage was applied, causing an electric-thermal effect on the GO film, which gave rise to the expansion of the compressed film. When the film was expanded, lubricant penetrated into the porous structure so that the surface switched from slippery (WSA around 2°) to non-slippery state (pining on the surface). The expansion of the GO film could be controlled by the applied voltage so

that the surface adhesion was also tunable (Figure 7h). Oh et al.[86] fabricated a SLIPS using a sandwich (i.e., an elastomeric membrane between two elastic electrodes) structured substrate which exhibited a dynamic variation in shape under varying voltage. The surface was in the slippery state when there was no voltage (Figure 7i). Applying the voltage gave rise to the inplane stretching of substrate. The rough structure without a covering of lubricant then appeared , causing the droplet to be pinned (Figure 7i). Taking advantage of such an electric responsive switch in surface adhesion, more complicated droplets manipulation was realised, such as oscillation (Figure 7j) and jetting (Figure 7k).

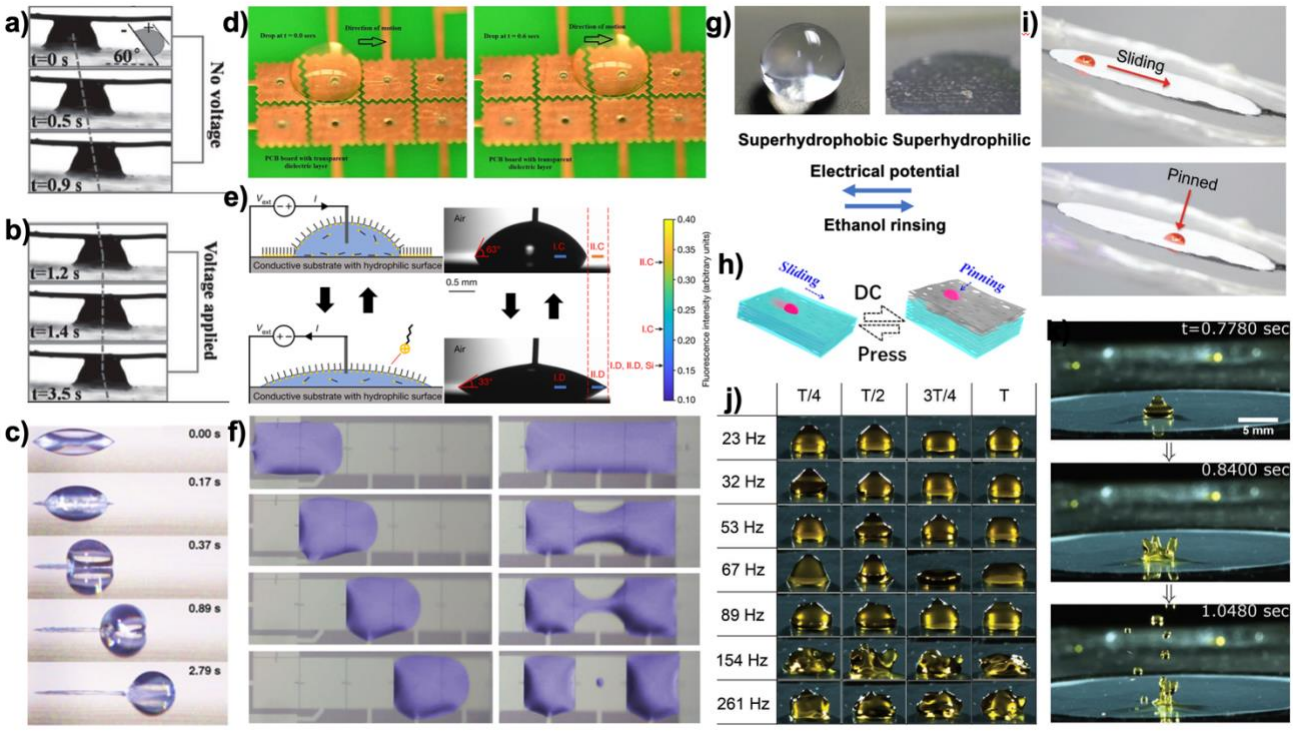

Figure 7. Electric response and the wetting on the surfaces (in air). a-b) Electrowetting; Reproduced with permission.[81] Copyright 2016, Wiley-VCH. c) Electric corona discharge controlled liquid behaviour; Reproduced with permission.[90] Copyright 2019, American Institute of Physics. d) On Cu electrode-embedded substrate, electric responsive fast moving of large ink drop; Reproduced with permission.[91] Copyright 2019, American Chemical Society. e-f) Electro-dewetting and its application on droplet directional moving, merging and splitting; Reproduced with permission.[84] Copyright 2019, Springer Nature. g) On a porous membrane with dodecyl chains, switch between superhydrophobic low adhesion and superhydrophilic; Reproduced with permission.[85] Copyright 2019, American Association for the Advancement of Science. h) On a SILPS using shape-memory graphene film as the substrate, switch between slippery state to non-slippery state; Reproduced with permission.[87] Copyright 2017, American Association for the Advancement of Science. i-k) On a sandwiched substrate, adhesion switch, droplet oscillation and jetting. Reproduced with permission.[86] Copyright 2018, Wiley-VCH.

Underwater environment

The underwater electro-responsive surfaces is useful for manipulating liquids/bubbles in various applications, such as microfluidics, oil recovery, printing/patterning drop control, and underwater antifouling, self-cleaning materials.

Wang et al.[88] proposed a strategy to achieve an insitu reversible adhesion transition between the underwater superoleophilic and superoleophobic states by constructing a binary textured surface. Taking the Cu/Sn composite system as an example, when closing and opening an external circuit, the reversible transition was realised (Figure 8a). The underlying principle was that the electrodeposited Sn layer caused a water-deficient layer by suppressing the hydrogen bonding network at the water/electrode interface, resulting in the diffusion of oil droplets on the surface. When the potential was removed, Sn was converted into Sn^{2+} and dissolved in the electrolyte solution again, and the composite surface system would gradually restore to a Cu-rich surface with high affinity for hydroxyl groups, which replaced the oil layer with aqueous electrolyte solution (Figure 8b). This material provides an new pathway for designing smart materials in the fields of liquid manipulating.

Polyaniline (PANI) is a conductive polymer, and there are some stable oxidation forms of it: semi-oxidized emeraldine base (EB) which could convert into emeraldine salt (ES) through a portion, fully oxidized pernigraniline base (PNB), and fully reduced leucoemeraldine base (LEB).[89, 94-99] Such a polymer could be employed for fabricating a responsive surface. For example, Ding et al.[89] prepared uniformly distributed PANI nanowire thin films (141.3±5.0 nm in length and 45.7±1.7 nm in diameter) through the aligned current deposition process. When a voltage of 0.43 V was applied to the PANI nanowire film, the OCA of 1,2-dichloroethane droplets in 0.1 mol/L $HClO_4$ solution (pH = 1.2)

on the surface is 161.61°±1.5° and the corresponding OSA was less than 3°, exhibiting superoleophobicity and a low oil adhesion in solution. When the voltage was adjusted to -0.2 V, although the surface still showed underwater superoleophobicity, its underwater OCA decreased to 154.2°±2.9°. No matter how the surface was inclined, the oil droplets are tightly adhered to the surface without slipping, indicating that the surface shows a high oil-adhesion state in the solution under this condition. When the applied potential was 0.8 V, the surface also exhibited superoleophobicity and high oil adhesion under water. Therefore, the underwater oil adhesion and wettability of the PANI membrane was controlled by adjusting the electrochemical potential. In terms of the internal mechanism of this phenomenon, the PANI nanowire film was in ES state when the external potential is 0.43 V, and protonation occursed at the nitrogen atom of the imine (generating polysemiquinone), thus the anion (ClO_4^-) had to act as a counter ion at the N^+ position to maintain charge neutrality. Therefore, the interaction between the surface and water molecules was enhanced, and the microstructure of the surface could be completely wetted by the electrolyte solution, giving the surface a high OCA and a low oil adhesion. But when the external potential decreased to -0.2 V or increased to 0.8 V, the PANI form changed from the ES state to the LEB or PNB state, and ClO_4^- was removed from the main chain of PANI, so that the interaction between PANI and water molecules was weakened. Consequently, the oil partially penetrated into the microstructure of surface, resulting in a high oil adhesion.

Tian et al.[100] showed a method of directionally driving underwater oil droplets by jointly controlling the surface (gradient structured porous polystyrene film) through the electric field and the gradient microstructure (Figure 8c). As shown in Figure 8d, the micropores on the surface gradually decreased from one edge to the others, showing a gradient distribution, and the corresponding underwater value

of OCA increased from 34° to 45°. They placed a liquid paraffin on the gradient surface immersed in water, where an unbalanced pressure force caused by the gradient of the membrane was generated at both ends of the droplet. This unbalanced pressure further made the shape of the two sides of the oil droplet asymmetric, having a specific tendency to move. When an electric field was applied, the contact area between the underwater oil droplet and the gradient structure porous membrane was reduced, thereby overcoming the original viscosity resistance of the oil droplet and the prepared surface. When the pressure difference generated by the gradient was greater than the viscous resistance of the membrane to the oil droplets, the underwater oil droplets could move from the large pore area on the surface to the small pore area (Figure 8e).

Liu et al.[101] developed a simple redox reaction using conductive polypyrrole (PPy) film to realise the intelligent switching between the high and low adhesion in terms of underwater oil droplets on the surface, and a potential wetting switch based on the oil/water/solid system was proposed. When a positive voltage was applied to the material, oil droplets adhered to the PPy surface. Conversely, when a negative voltage was applied, the adhesion force of the oil droplets on the surface of the material decreased, so it starts to roll under the influence of gravity, showing different droplet behaviour.

Finally, Yan et al.[83] revealed a unidirectional manipulation strategy for underwater oil droplets or bubbles on the surface of copper wire coated with porous polystyrene (PS) film by combining electrowetting induced adhesion conversion and the gravity/buoyancy of oil droplets/bubbles (Figure 8f). The as-prepared porous PS film coated copper wire was able to capture and maintain oil droplets or bubbles underwater without applying voltage. When the applied voltage increased, the wettability of the surface by water also increased, so the adhesion of underwater oil droplets or bubbles on the surface was decrease (Figure 8g, 8h). Depending on the relative density, underwater oil

droplets/bubbles could move unidirectionally downward/upward on the surface at a voltage greater than their critical voltage (Figure 8i). Otherwise, underwater oil droplets or bubbles firmly adhered to the surface of the porous PS membrane (Figure 8i).

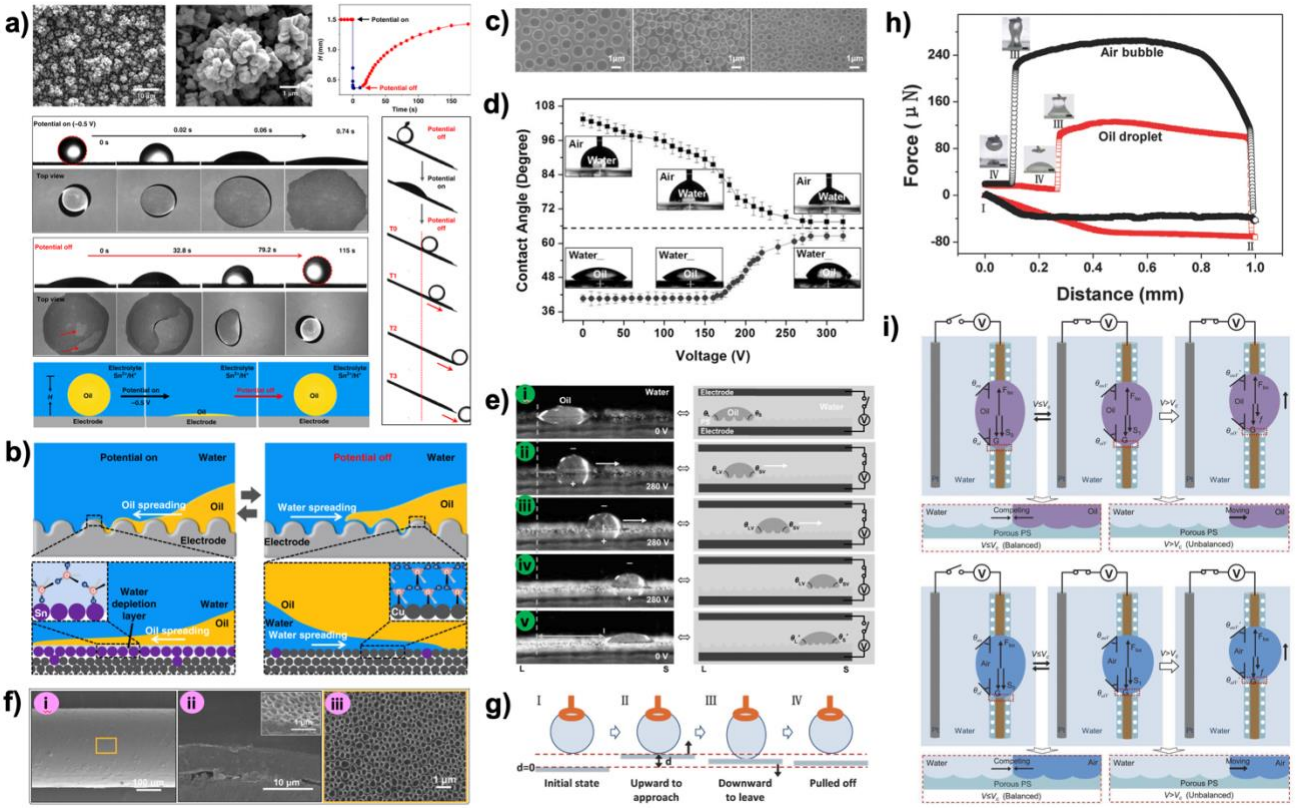

Figure 8. Electric response on smart surfaces (under water). a, b) Cu/Sn composite surface: Reproduced with permission.[88] Copyright 2020, Springer Nature. a) In situ reversible superwettability transition between underwater superoleophilicity and superoleophobicity. b) The schematics show that the Cu/Sn binary composite surface enables drastic altering of the hydrogen bonding network at the electrolyte/electrode interface, making the oil droplet experience the in situ reversible transition between superoleophobicity and superoleophilicity. c-e) Porous PS film: Reproduced with permission.[100] Copyright 2016, Wiley-VCH. c) Morphology characterization of the gradient structured porous polystyrene (PS) film. d) CA change for water and underwater oil droplets as functions of the applied voltage on the porous PS film surface. e) Electric field and gradient microstructure cooperate to drive directional motion of an un-derwater oil droplet. f-i) Porous PS films on copper wire. Reproduced with permission.[83] Copyright 2018, Wiley-VCH. f) Morphology characterization. g, h) Adhesion characterization. i) Schematics of the wetting states of an underwater oil droplet (liquid paraffin) or air bubble on the porous PS film-coated copper wire surface under an applied electric field.

3.5 Photo-responsive surfaces

Atmospheric environment

The studies on photo-responsive surfaces worked on either atmospheric or underwater environment have capturing increasing attentions during recent years. Photo-responsive surfaces not only have some traditional applications (e.g. fog-harvesting, microfluidics, liquid transport, water/oil seperation) the same as other types of responsive surfaces, but also could potentially be used for boarder application such as photocatalysis and microreactor.

The photo response (Figure 9) can realise the remote control of surface wettability and adhesion without direct contact or introducing electrodes.[102, 103] Therefore, compared with other responsive surfaces, more modes of switch in wettability and adhesion can be realised (Table 6). Furthermore, both inorganic and organic materials (Table 6) can be designed to be a photo responsive surface, but each will have a different mechanism.

Table 6. Advantages and diversity of photo-responsive/light-driven surfaces (in air and underwater)

Advantages	**Details**	**Ref.**
Diverse types of materials of interface can be used	nano metallic oxides/ semiconductor e.g. ZnO, TiO_2, SnO_2	[104-117]
	photoactive polymers e.g. Azobenzene based polymer	[118, 119]
All modes of switch in surface properties can be realised	SA change as CA switch, switching between (super-)lyophilic and slippery state	[108, 112, 120, 121]
	CA switch without SA change	[110]
	SA switch without CA change, switching between pinning and slippery state	[117]

	Switching amongst lyophilic, slippery, and pinning state	[111]
	Switching between isotropic and anisotropic state	[118]
Diverse control avenues are feasible	UV illumination	[108, 112, 113, 115, 120, 122, 123]
	UV light through a photomask	[111]
	Linearly polarized light irradiation	[118]
	Infrared-light irradiation	[119]
	Varying the distribution, duration, or the power of light irradiation	[116, 118, 119]
	To switch back: put in the dark	[112]
	To switch back: heat treatment	[111, 114]
	To switch back: chemical treatment	[115]

Similar to the mechanism of semiconductor materials, the surface energy of various nano metallic oxides can be easily changed by illumination.[103] For example, ZnO nanoarrays were formed on the materials, where the surface micro/nano-structures were changed and the photo response under ultraviolet (UV) illumination was achieved.[120, 122, 123] Such a response could reversibly switch the wettability between superhydrophobic and superhydrophilic.[120, 121] Researchers also found that TiO_2, SnO_2 could possess similar performance.[104-107] Contrary to conventional nanoarray decoration, Malm et al.[108] developed an atomic layer deposition method, by which an ultrathin ZnO layer was coated on a superhydrophobic cicada wings. This coating made minimal variation to the surface topography but remarkably changed the surface chemistry. The WCA on such a ZnO coating is photo responsive. As shown in Figure 9a, the surface maintained a superhydrophobicity after the ZnO coating. Under UV illumination, the WCA decreased sharply from around 160° to 14° (Figure 9b,c). The amplitude of the CA variation was also controllable by optimizing the ZnO deposition cycle (Figure 9c). Such a hydrophilic ZnO coating could recover superhydrophobicity when stored at 100°C in the absence of light. The above studies were based on the observation that a wettability switch brings

about an associated adhesion switch. Recently, Han et al.[109, 110] developed a ZnO composite SLIPS which had photo-electric cooperative response. On such a surface, could they realised a reversible switch of CA without an SA change, as shown in Figure 9d.

The surface adhesion property switch between superhydrophobic low and high adhesion could also be controlled on photo-responsive metallic materials.[117] Li et al.[111] sprayed a ZnO nanoparticle suspension onto a substrate. As shown in Figure 9e, the WCA was 162° and SA was 2° after spraying, showing a superhydrophobic low adhesion property. When the surface was irradiated by UV light through a photomask, it transformed from low adhesion to very high adhesion where the droplet was pinned, without changing the superhydrophobic property (Figure 9f). The corresponding adhesion force ranged from 5.1 μN to 136.1 μN (Figure 9e-f). When the surface was under UV illumination without a mask, it become a hydrophilic surface (Figure 9g). Through UV irradiation and heat treatment, the reversible transformation amongst superhydrophobic low adhesion, superhydrophobic high adhesion, and hydrophilic could be realised. Velayi et al.[114] further studied how the annealing temperature in the heat treatment affected the switch in wettability and adhesion property.

Another approach to studying photo responsive surfaces which has developed rapidly in recent years has been to employ photoactive polymers. The photo response of polymers results from chromophore photoisomerization or the photothermal effect.[102, 124-130] Azobenzene is a typical example of photochromic molecule.[131, 132] The shape of a polymer containing azobenzene can be varied under different lighting conditions.[133-135] For example, Gao et al.[118] decorated the surface of substrates with photo responsive poly[6-(4-methoxy-4’-oxyazobenzene)hexyl methacrylate] microsphere arrays. The substrate was initially treated to a lotus leaf state with isotropic superhydrophobicity. After irradiation using linearly polarized light (LPL), the microspheres transformed into an ellipsoid shape.

As shown in Figure 9h, the surface remained highly hydrophobic but exhibited anisotropic adhesion. The WSA for droplets moving parallel to the longer axes of the ellipsoid was 3° but the SA for moving vertically was 18°. As shown in Figure 9h,i, enhancing the exposure time to LPL increased the degree of anisotropy of the adhesion so that the surface could change from lotus leaf state to rice leaf state. They explained the adhesion change by TPLC switching from the totally disrupted state to the anisotropic continuity state. Additionally, polymers which contain anthracene, stilbene, acetoxystyrene are also good candidates for photo response smart surface.[102, 136, 137]

By adding photothermal substances into polymers they can respond under light due to the photothermal effect.[138] For instance, Gao et al.[119] embedded photothermal Fe_3O_4 nanoparticles in a lubricant-infused PDMS organogel and achieved a photothermal responsive smart surface. When a local infrared-light irradiation was exerted on the surface, a dynamic temperature gradient formed, as shown in Figure 9j. The gradient gave rise to an imbalance between the advancing and receding angle so that the droplet could move (Figure 9j). By varying the distribution and the power of light irradiation, the retention force against droplet moving towards different direction was optimized artificially, enabling the water droplets to move to a desired location at the desired speed or acceleration (Figure 9k).

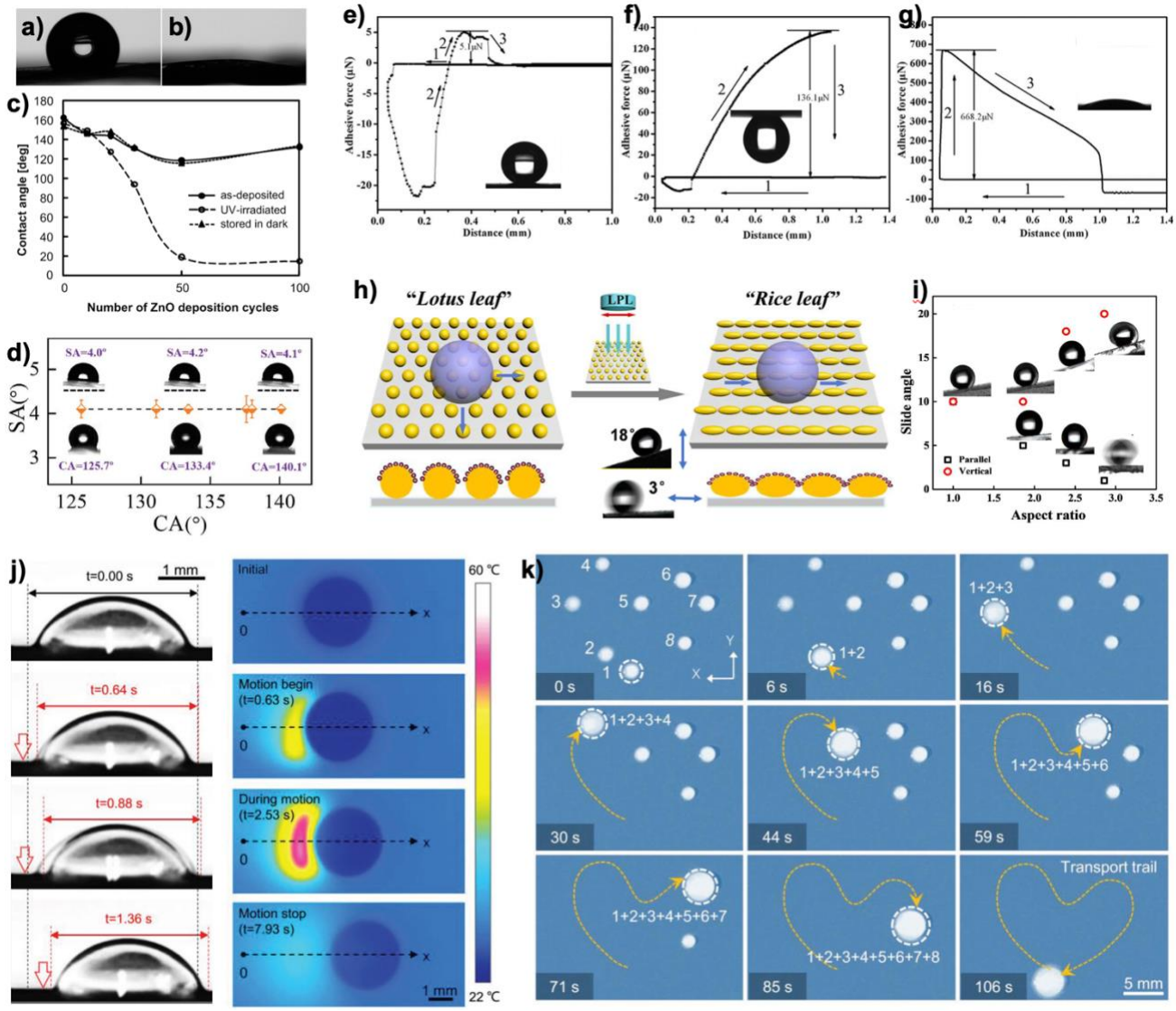

Figure 9. Photo response or light driving on surfaces (in air). a-c) On a ZnO ALD-coated surface, WCA switch between superhydrophobicity and nearly superhydrophilicity; Reproduced with permission.[108] Copyright 2010, American Chemical Society. d) On a ZnO-composite SLIPS, CA switch without SA change; Reproduced with permission.[110] Copyright 2019, Wiley-VCH. e-g) On a ZnO nanoparticle suspended surface, CA or/and adhesive force switch amongst superhydrophobic low adhesion, superhydrophobic high adhesion, and hydrophilic; Reproduced with permission.[111] Copyright 2014, Elsevier Ltd. h-i) On an azobenzene-contained microsphere array structured surface, adhesion property switch from lotus leaf state to rice leaf state; Reproduced with permission.[118] Copyright 2018, American Chemical Society. j-k) On a Fe_3O_4 nanoparticles embed lubricant-infused PDMS organogel, droplet manipulation due to photothermal response induced retention force difference. Reproduced with permission.[119] Copyright 2018, Wiley-VCH.

Underwater environment

As mentioned above, UV light could finally affect the interaction of some water/solid interfaces. When it comes to the underwater environment, the influence on water of surface structures or chemistry

change is linked to the water/oil/solid interface, which exerts a significant effect on the oil droplet behaviour (Figure 10).

For example, Yong et al.[116] constructed a new type of multi-layered TiO_2 surface with switchable wettability by femtosecond laser etching of titanium plates (Figure 10a). After being immersed in water, the surface reflected uniform light in the TiO_2 area like a silver mirror. This phenomenon was caused by the air band between the water and the substrate.[139] Oil droplets quickly spread over the underwater interface when they touched the rough structure (OCA=4°), which indicated that the laser-treated TiO_2 surface was underwater superoleophilic (Figure 10b). After UV irradiation for 40 minutes, the surface exhibited totally different wettability (OCA=160.5°±2°). Meanwhile, the silver mirror-like reflected light disappeared, showing that water replaced the original air band to wet and fill the gaps of micro/nano structures on the TiO_2 surface. The filled water layer was repellent to oil, which enabled the surface to exhibit superoleophobicity under water. They also found that after placing the sample in dark air for two days, the initial underwater superoleophilicity reappeared; the above two states had repeatable characteristics (Figure 10b). This reversible switch was based on the UV-sensitivity of TiO_2.[112, 140] When TiO_2 surface was exposed to UV light, a large number of electron pairs and holes were formed on the surface. The generated holes would further combine with the lattice oxygen to form highly unstable oxygen vacancies. Each oxygen vacancy dissociated water molecules to generate two adjacent Ti-OH groups. Due to the hydrophilicity of the -OH group, water was able to completely wet microstructures when UV treated TiO_2 surface was immersed in water. When the surface was placed in dark air, the hydroxyl groups generated by the dissociation of oxygen vacancies were replaced by oxygen in the air, restoring the surface to its original underwater superoleophilicity (Figure 10 c).[112]

Wang et al.[115] used hydrothermal method on a fluorine-doped tin oxide substrate to fabricate a uniformly distributed rutile-type TiO_2 flower with an layered structure in a diameter of about 6 μm. The structured surface exhibited superoleophobicity in water (OCA =155°). The surface had a low oil adhesion due to the formation of a fish scale-like solid/water/oil system in which water molecules were trapped in the TiO_2 microstructures and formed water layer showing oil repellency. However, when the sample was contaminated with oleic acid (e.g., 0.5 wt% in n-pentane for 5 s), it lost the underwater superoleophobicity (the OCA decreased to 64°). This was mainly because during the process of oleic acid contamination, some oleic acid spots were also trapped in the microstructure of the TiO_2 surface, so that the droplets on the TiO_2 surface were in a non-uniform adhesion state. The oleic acid spots in the microstructure caused the reduction of contact area between the water and the oil droplets in the microstructure, thus decreasing the underwater OCA. Interestingly, when the surface was irradiated with UV light for 2 h, the original underwater superoleophobicity recovered. The recovery occurred because electron-hole pairs generated on the UV treated TiO_2 surface. These holes adsorbed water molecules around the interface and produced hydroxyl radicals that were highly susceptible to reaction. The hydroxyl groups further oxidized and decomposed organic compounds such as oleic acid, which made TiO_2 surface return to superhydrophobic.

Shami et al.[113] further reported a 3D reversible wettability PVDF-P25TiO_2 nano-textured surface, which was prepared by electrospinning using PVDF and P25TiO_2 as raw materials (Figure 10d). The light-induced superhydrophilic & underwater oleophobic properties of the composite surface played an important role in the oil/water separation. During the separation process, the water in the mixed liquid was able to quickly pass through the surface due to the superhydrophilic property of the surface. When the oil reached the surface, it would be blocked at one side of the surface because of the

underwater superoleophobic property, achieving water separation (Figure 10d). In addition, the water on the surface could be removed by a simple heat treatment after the separation operation, therefore the surface was reusable.

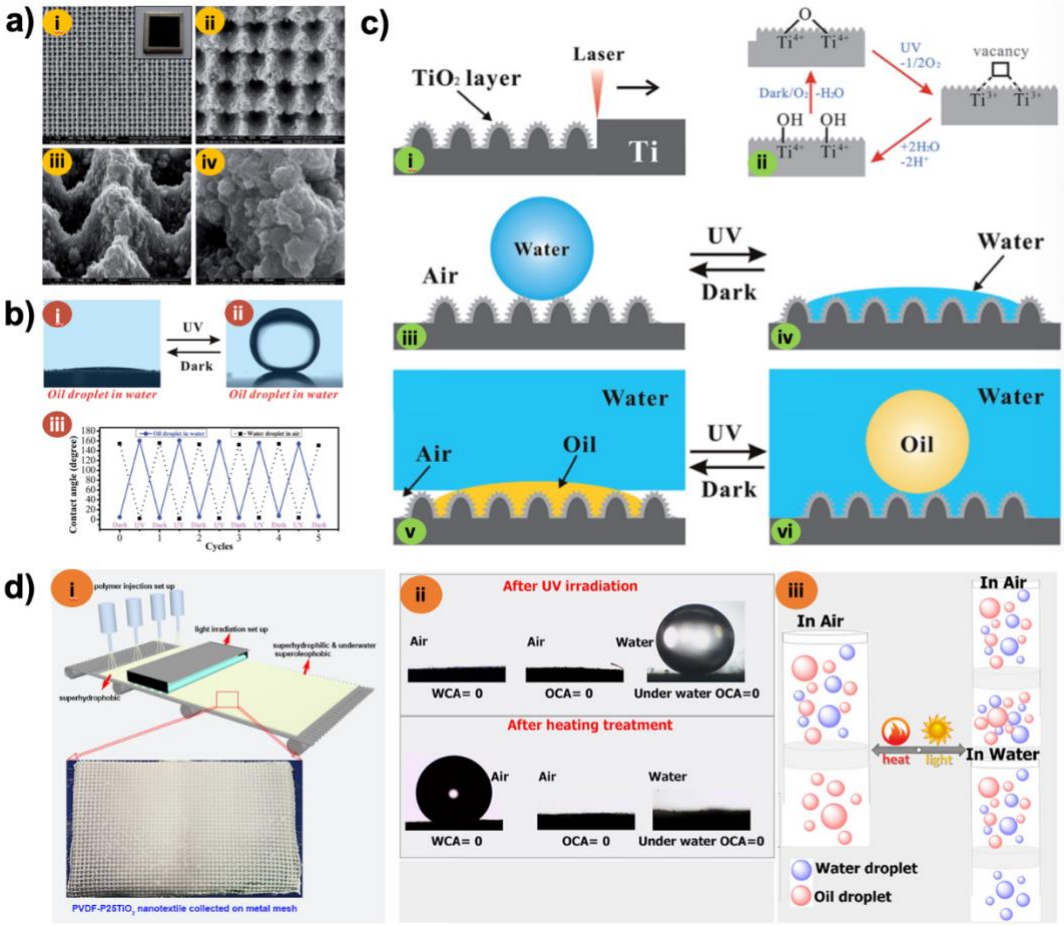

Figure 10. Photo response on smart surfaces (under water). a-c) TiO_2 surface: Reproduced with permission.[116] Copyright 2015, The Royal Society.a) SEM images of the rough Ti surface after femtosecond laser ablation. Reproduced with permission. b) Underwater oil droplet on the rough sample surface after i) storing in the dark, ii) irradiation with UV light and iii) Alternation of the above dark and UV light, respectively. c) Schematic illustration of the switchable wettability. d) Schematic illustration of large-scale fabrication process of the As-Spun nanotextileand as well as the schematic illustration of the photo/heat-induced wetting behaviour for this surface. Reproduced with permission.[113] Copyright 2020, American Chemical Society.

3.6 Humidity-responsive surfaces

Humidity can be considered a dependent variable which can affect droplet behaviour. In nature, many plants respond to the changes in humidity by adjusting either their water absorption or

evaporation.[141-143] On some specific bio-inspired micro/nano-structured surfaces, the surface wettability and adhesion may also vary when they are exposed to different levels of humidity.

Recently, Qu et al.[144] discovered that the porous nanostructure of a peanut leaf could automatically respond to humidity changes (Figure 11a-c). When the ambient relative humidity was lower than the saturated humidity (namely RH<99%), as shown in Figure 11a, the surface showed a superhydrophobic high adhesion property, with a WCA approximately 150° and an adhesive force of about 40 μN (Figure 11c). When the RH>99%, the surface suddenly switched to a superhydrophilic state (Figure 11b) owing to the humid air filling the nanoscale framework. The WCA decreased dramatically to below 10°, showing a switch from superhydrophobicity to superhydrophilicity. Inspired by the peanut leaf, they fabricated a humidity responsive metal-organic framework (MOF) which had a similar performance (Figure 11d-f). This smart surface also showed a switch from superoleophilicity to superoleophobicity/underwater superoleophobicity (Figure 11f) due to the formation of a water film when the RH increased.

In the same way that the humidity responsive formation of a water film can enable a surface to be more oleophobic and hydrophilic with high water adhesion, the break of a water film can also relate to the switch in the surface adhesion property. Recently, Li et al.[145] developed a ZnO-nanocone decorated 3D multi-intersectional fibre network, (Figure 11g) and found that the surface adhesion switched during the application of fog-water harvesting. As shown in Figure 11h, the original web was hydrophobic with medium water retention force (around 800 μN). After hydrophilic ZnO-nanocone decoration, the web was more attractive to water and the retention force against water gathering become higher. When the web was exposed to humid air, the retention force decreased dramatically from 2090 μN to 230 μN after being wetted, accelerating the water movement for collection. They

explained this smart switch by a humidity induced Rayleigh Instability break in the water film (Figure 11i): the unique web which had 3D multi-intersectional structure together with hydrophilic nanocone array decoration.[146-148]

The humidity response induced switch in surface wettability, adhesion and droplet behaviour is potentially an exciting research field, where on the interface the water (droplet) is affected by water (moisture). In addition, the underwater state could be regarded as an extremely humid condition, where the moisture/water exert maximum influence upon the interface.

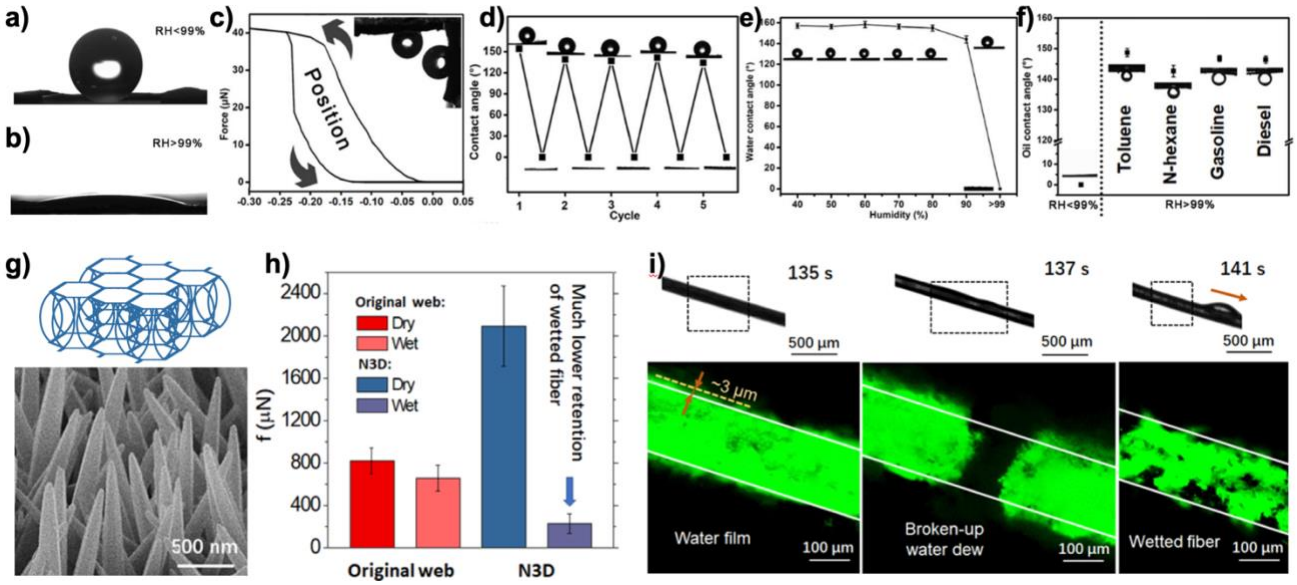

Figure 11. Humidity response on smart materials (in air). a-c) On a peanut leaf, WCA switch between superhydrophobicity and superhydrophilicity; d-f) On a peanut leaf inspired MOF, water and OCA switch between superhydrophobicity/superoleophilicity and superhydrophilicity/superoleophobicity; Reproduced with permission.[144] Copyright 2020, American Chemical Society. g-i) On a nanocone-decorated 3D multi-crossing fibre network, surface adhesion property switch from high retention force to low retention force. Reproduced with permission.[145] Copyright 2019, American Chemical Society.

3.7 pH-responsive surfaces

A variation in pH can also change the underwater surface wetting and oil adhesion. pH-responsive surfaces could adjust the contact conditions by the solution pH, which allowes the surface to effectively

capture and release the oil droplet in solution. This makes it applicable to the field of marine oil pollution treatment.

Cheng et al.[149] prepared a surface that was able to adjust the wettability of underwater oil through pH by assembling $HS(CH_2)_9CH_3$ and $HS(CH_2)_{10}COOH$ on the substrate surface (Figure 12a). The surface showed superoleophilicity in a neutral or acidic aqueous solution (pH≤7), on which the underwater OCA (octane, 4 μL) was constant at 0°. But when the surface is placed in an alkaline solution, its underwater OCA value increased as the pH. When the pH of the solution reached 12, the surface showed superoleophobicity (OCA =162°) in the water (Figure 12b). Experiments found that after the sample surface was removed from the alkaline solution and washed with deionized water, and then immersed in an acidic liquid again, it would return to underwater superoleophilicity. This reversible transition between the underwater superoleophilic state and the superoleophobic state can be repeated multiple times. The inherent reason for the above switchable wettability was the uniform distribution of carboxylic acid groups and alkyl groups on the surface of the sample, where the carboxylic acid groups would be protonated in acidic solutions and deprotonated in alkaline solutions. Therefore, when the surface was placed in a neutral or acidic solution (pH≤7), the alkyl group on the sample surface dominated, enabling the surface to have lower surface free energy, so it showed superoleophilicity in water. In contrast, under alkaline solutions, the surface carboxylic acid groups are deprotonated (Figure 12c). The deprotonated state was hydrophilic, allowing water molecules to be trapped in the rough structure. The higher the pH, the higher the degree of deprotonation of the carboxylic acid group. When the pH of the solution was higher than 12, the surface microstructure was able to capture a sufficiently thick water layer, thereby forming a stable solid/water/oil three-phase system leading to underwater superoleophobicity.

Inspired by the micro/nano-structure of fish scale, Huang et al.[150] prepared a pH-responsive underwater superoleophobic film by combining in-situ anodic aluminum oxide (AAO) template polymerisation and polymerisation modification (Figure 12d). The surface of the film was composed of polypentafluorophenyl acrylate micropillars grafted with polymethacrylic acid nano-brushes. The structure enabled the film surface to have a micro/nano-scale layered structure, which not only kept the surface superoleophobic in water, but also enabled the surface to adjust oil adhesion (Figure 12e, f). Under acidic conditions, oil droplets could remain on the surface and exhibited the pinning state. If the solution turned to neutral or alkaline conditions, the oil droplets on the surface would turn into the slippery state where free sliding of oil drops occurred on the surface (Figure 12g). Based on the underwater sliding oil angle in response to pH, the surface could be reversibly switched between low and high oil tightness.

Zhang et al.[151] designed underwater smart surfaces by grafting pH-responsive P2VP-b-PDMS (P2VP: Poly(2-Vinylpyridine)) on non-woven textiles and sponges. For the grafted P2VP block, it could change surface wettability and conformation through protonation and deprotonation in response to the pH value of the aqueous medium. The oleophilic PDMS block grafted on the surface could control the oil droplet entry, and further provided a controlled oil entry route through the oleophilic PDMS block, thereby regulating the oil wettability of the surface in water.

In addition, Cheng et al.[152] grafted a pH-responsive PAA layer on a glass substrate by a plasma polymerization method. The underwater adhesion of the grafted PAA film to oil droplets was regulated by the pH of the solution. As the pH gradually increased from 1.0 to 12.0, the adhesion of the surface to underwater oil droplets gradually decreased from 21.6±5.0 μN to 0 μN. If the surface was placed in a low pH solution again at this time, the adhesion between the surface and the oil increased again, and

the switching between the different states described above was repetitive. They also found that the adjustable oil adhesion possessed by the surface was caused by the chemical composition (pH-dependent) and micro/nano roughness of the surface. When the pH of the solution was less than 4.7, adjacent carboxylic acid groups on the PAA chain could form intramolecular hydrogen bonds, and the conformation of the PAA molecule was in a coiled state, thus the proportion of water on surface became low. The oil droplets could then be in contact with the surface rough micro-structure. In this case, the surface had an underwater OCA of less than 150° and an extremely high adhesion to oil droplets. When the pH of solution was higher than 4.7, the intermolecular hydrogen bonds were formed between the carboxylic acid group on the PAA branch and the water molecules in the solution, and the conformation of the PAA molecule became stretched. Also, the intermolecular hydrogen bond made the proportion of water on surface higher, forming a water layer between the surface and the oil droplet, which provides repulsive force for the oil showing a high adhesion.

We can know that all the above pH-sensitive surfaces are grafted with one or more polymer materials that could respond to pH. When the pH of the solution changes, the functional groups/molecules on the surface would also change, resulting in the variation of underwater wetting and adhesion of oil droplet.

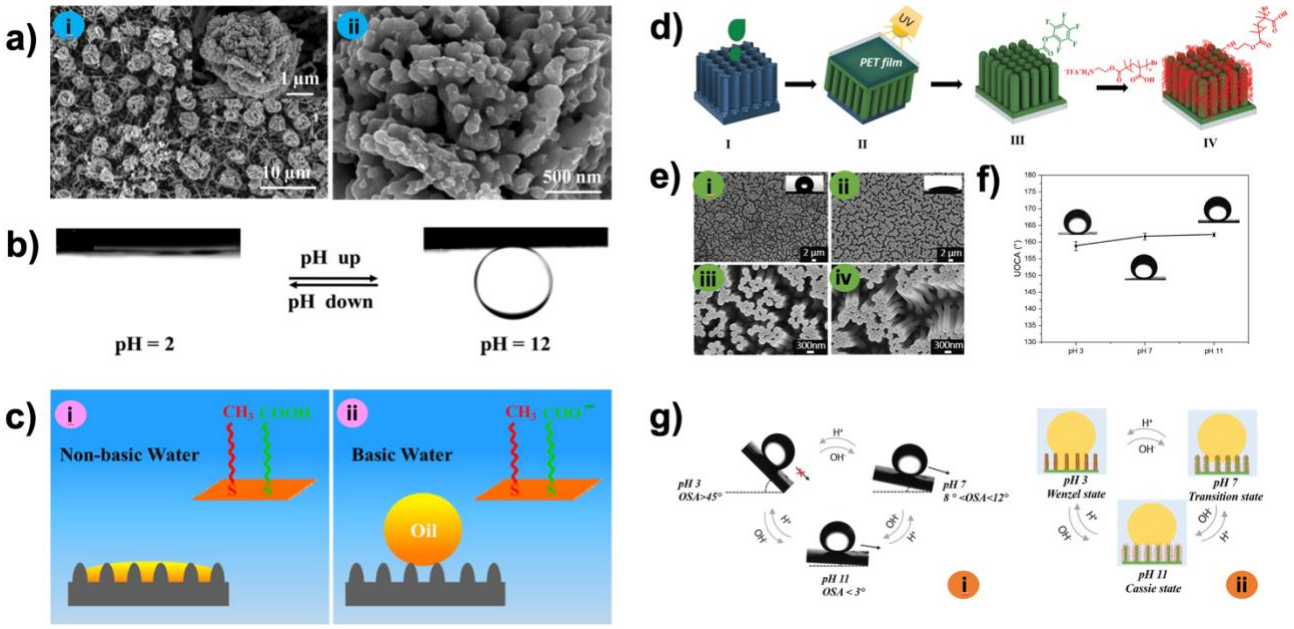

Figure 12. pH response and the liquid behaviour (under water) on surfaces. a-c) $HS(CH_2)_9CH_3$ and $HS(CH_2)_{10}COOH$ composite surface: Reproduced with permission.[149] Copyright 2014, American Chemical Society. a) SEM images of the artificial surface assembled of $HS(CH_2)_9CH_3$ and $HS(CH_2)_{10}COOH$. b) Wettability of oil droplet in acidic (pH = 2) and basic (pH = 12) solution, respectively. c) Schematic illustration of the responsive oil wettability on the rough surface. d-g) PPFPA-g-PMAA surface: Reproduced with permission.[150] Copyright 2020, Wiley-VCH. d) Schematic illustration of fabrication procedures. e) FE-SEM and magnified images of PPFPA micropillars and PPFPA-g-PMAA. f) Underwater oil contact angle (UOCA) values and corresponding images of pillar-PPFPA-g-PMAA surface at different pH values. g) Schematic illustration of underwater oil droplet on the pillar-PPFPA-g-PMAA surface.

4. Summary & Outlooks

Smart surfaces can respond to stretching, magnetic, photo, electric, temperature, humidity, and pH. These smart surfaces utilise either a single response or multiple responses to these stimuli. Reviewing the studies on diverse stimuli-responsive switchable-adhesion surfaces working in atmospheric or underwater environment, the following conclusions may be drawn. Firstly, the contact conditions between a surface and a liquid can be divided into four states in either atmospheric or underwater environment, i.e., lyophilic, pinning, slippery, and anisotropic state. Responsive smart surfaces are able to reversibly switch from one contact state to at least another one state under external stimuli.

Secondly, for artificial stimuli-responsive surfaces, the chemical component, chemical distribution, surface topography, or/and parameter of environmental phase are changed when exposed to external stimuli. The wettability, adhesion, and/or the contact state of the surface are therefore transformed, leading to changes in the liquid behaviour. By further varying the parameter of the external stimuli through diverse control avenue, various modes of liquid behaviour can be realised, e.g. droplet deformation, unidirectional motion, bouncing, splitting.

Although great progress has been achieved in the development of responsive smart surfaces systems, many fundamental and practical challenges remain for this technology to find widespread applications. As for the future studies, herein we propose different suggestions for some fields where smart surfaces are employed:

In terms of the research and application of accurate droplet manipulation, to fully understand the mechanisms of chemical or topographic effects on surface adhesion, researchers should ensure that the effects caused by other factors will not influence the results. For example, in the studies on temperature-responsive surfaces, micro/nano-structures on a surface were transformed when the surface was heated. However, the temperature of the liquid under investigated might also be changed, which may leading to change in some properties of the liquid.[153] Researchers should try to minimise the influence of this change when evaluating how stimuli-induced nanostructure variation affects liquid behaviour.

In terms of the research on fluid mechanics and fluid control, the behaviour of other types of liquids (e.g. non-Newtotian fluids) [154] on the surfaces should be studied. In the majority of the current studies, behaviour of only water and light oil has been studied systematically. Either water or light oil is a Newtoian fluid. However, the non-Newtoian fluids (e.g. biofluid, some saline solutions, some

polymeric solutions) show different trends of behaviour in response to external forces especially on hydrophilic surfaces.[155] Only when the behaviour of non-Newtoian fluids are widely investigated can more potential applications of smart surfaces become practical.

In terms of the application in medical and pharmaceutical domains, designing soft wearable device is a promising industry. A challenge is to link the ability of a surface to realise liquid response with the ability of a surface to adhere to human skin. Most existing studies on smart wearable device are carried out when the skin is dry. Few studies has investigated how the sweat or other liquid skin-secretion affected the ability of surface to adhere to human skin.[156] The controllable responsive surface can be employed when these studies are carried out. In addition, we appeal that further studies which aim to promote smart surfaces application in bio-medical fields should use materials in good biocompatibility as substrates.

To promote the practical application of smart surfaces used for liquid transport, fog harvesting, reactor, or other purposes in hydraulic and chemical engineering fields, researchers should explore methods to prepare relatively large-scale surfaces with low cost. The durability of such a surface working in practical conditions should also be investigated.

To open the door for wider practical application, we suggested that stimuli-responsive surfaces can be combined with the concept of bio-inspired hybrid or Janus interface,[157] which have wettability gradient. The reported artificial responsive surfaces mostly had continuous wettability and switched between different continuous states. From our perspective, a wettability-gradient material can be employed as a substrate when a stimuli-responsive surface is designed. A stimuli-responsive hybrid/Janus interface may realise reversible switch in the direction or even the disturbation of the gradient. Therefore, more factors related to interfacial property and liquid behaviour can be more

accurately controlled. Such combination may lead to emerging applications such as smart clothing. For example, such an interface is able to realise accurately controllable absorption and ejectment of sweat, heat and air, while it is hard for either single stimuli-responsive surfaces or single hybrid/Janus interfaces to realise all these goals.

We firmly promote the view that designing artificial stimuli-responsive smart surfaces is a promising research and commercial field. The development of such smart surfaces is in the ascendant and show diversity. Various responses can be designed and diverse materials can be employed. Multifunctional surfaces can be made using common materials. Smart surfaces have potential applications in numerous fields, such as microfluidics manipulation, liquid transport/harvesting, thermal/energy management, and flexible intelligent device design relating to the fields of biomedical devices, electronics, chemical engineering and many more.

Acknowledgements

The strong support from the Aviation Industry Corporation of China (AVIC) Manufacturing Technology Institute (MTI) for this funded research is much appreciated. This work is mainly performed at the AVIC Centre for Structural Design and Manufacture at Imperial College London. This work was also supported by the EPSRC Program Manufacture Using Advanced Powder Processes (MAPP)EP/P006566. Chang Li was also supported by China Scholarship Council (No.202008060076). Ming Li acknowledges financial assistance from Imperial College London granting him the “President Scholarship”. Qingwen Guan acknowledges the support from China Scholarship Council (No.202006440011).

Author contributions

Chang Li and Ming Li conceived, designed, and executed this project; they contribute equally to this work. Zhongshi Ni and Qingwen Guan assist the writing and revision of the manuscript. Bamber Blackman and Eduardo Saiz revised the language of the entire manuscript; they also provided useful suggestions for the revision, especially the summary & outlook section.

Conflict of interest

The authors declare that they have no conflict of interest.

References

[1] Tian, Y., Su, B. & Jiang, L. 2014 Interfaces: Interfacial Material System Exhibiting Superwettability (Adv. Mater. 40/2014). *Adv. Mater.* **26**, 6871-6871.
[2] Li, M., Xu, Q., Wu, X., Li, W., Lan, W., Heng, L., Street, J. & Xia, Z. 2018 Tough reversible adhesion properties of a dry self-cleaning biomimetic surface. *ACS Appl. Mater. Inter.* **10**, 26787-26794.
[3] Shang, L., Cheng, Y. & Zhao, Y. 2017 Emerging droplet microfluidics. *Chem. Rev.* **117**, 7964-8040.
[4] Zhang, P., Lin, L., Zang, D., Guo, X. & Liu, M. 2017 Designing Bioinspired Anti-Biofouling Surfaces based on a Superwettability Strategy. *Small* **13**, 1503334.
[5] Ding, Y., Tu, K., Burgert, I. & Keplinger, T. 2020 Janus wood membranes for autonomous water transport and fog collection. *J. Mater. Chem. A* **8**, 22001-22008.
[6] Peppou-Chapman, S., Hong, J.K., Waterhouse, A. & Neto, C. 2020 Life and death of liquid-infused surfaces: a review on the choice, analysis and fate of the infused liquid layer. *Chem. Soc. Rev.* **49**, 3688-3715.
[7] Tian, D., Guo, Z., Wang, Y., Li, W., Zhang, X., Zhai, J. & Jiang, L. 2014 Phototunable Underwater Oil Adhesion of Micro/Nanoscale Hierarchical-Structured ZnO Mesh Films with Switchable Contact Mode. *Adv. Funct. Mater.* **24**, 536-542.
[8] Xu, W., Zheng, H., Liu, Y., Zhou, X., Zhang, C., Song, Y., Deng, X., Leung, M., Yang, Z. & Xu, R.X. 2020 A droplet-based electricity generator with high instantaneous power density. *Nature* **578**, 392-396.
[9] Zhang, P., Chen, S., Zhu, C., Hou, L., Xian, W., Zuo, X., Zhang, Q., Zhang, L., Ma, S. & Sun, Q. 2021 Covalent organic framework nanofluidic membrane as a platform for highly sensitive bionic thermosensation. *Nature Communications* **12**, 1-7.
[10] Zhang, J., Wang, J., Zhao, Y., Xu, L., Gao, X., Zheng, Y. & Jiang, L. 2008 How does the leaf margin make the lotus surface dry as the lotus leaf floats on water? *Soft Matter* **4**, 2232-2237.
[11] Zhang, M., Feng, S., Wang, L. & Zheng, Y. 2016 Lotus effect in wetting and self-cleaning. *Biotribology* **5**, 31-43.
[12] Feng, L., Zhang, Y., Xi, J., Zhu, Y., Wang, N., Xia, F. & Jiang, L. 2008 Petal effect: a superhydrophobic state with high adhesive force. *Langmuir* **24**, 4114-4119.
[13] Bixler, G.D. & Bhushan, B. 2013 Fluid drag reduction and efficient self-cleaning with rice leaf and butterfly wing bioinspired surfaces. *Nanoscale* **5**, 7685-7710.
[14] Cai, Y., Lin, L., Xue, Z., Liu, M., Wang, S. & Jiang, L. 2014 Filefish-inspired surface design for anisotropic underwater oleophobicity. *Adv. Funct. Mater.* **24**, 809-816.
[15] Liu, X., Zhou, J., Xue, Z., Gao, J., Meng, J., Wang, S. & Jiang, L. 2012 Clam's shell inspired high-energy inorganic coatings with underwater low adhesive superoleophobicity. *Advanced Materials* **24**, 3401-3405.
[16] Hao, C., Liu, Y., Chen, X., Li, J., Zhang, M., Zhao, Y. & Wang, Z. 2016 Bioinspired interfacial materials with enhanced drop mobility: From fundamentals to multifunctional applications. *Small* **12**, 1825-1839.
[17] Lu, H., Zhang, M., Yang, Y., Huang, Q., Fukuda, T., Wang, Z. & Shen, Y. 2018 A bioinspired multilegged soft millirobot that functions in both dry and wet conditions. *Nat. Commun.* **9**, 1-7.
[18] Zhao, Y., Wu, Y., Wang, L., Zhang, M., Chen, X., Liu, M., Fan, J., Liu, J., Zhou, F. & Wang, Z. 2017 Bio-inspired reversible underwater adhesive. *Nat. Commun.* **8**, 1-8.
[19] Adamson, A.W. & Gast, A.P. 1967 *Physical chemistry of surfaces*, Interscience publishers New York.
[20] Yoon, R.-H., Flinn, D.H. & Rabinovich, Y.I. 1997 Hydrophobic interactions between dissimilar surfaces. *J. Colloid Interf. Sci.* **185**, 363-370.

[21] Guo, C., Wang, S., Liu, H., Feng, L., Song, Y. & Jiang, L. 2008 Wettability alteration of polymer surfaces produced by scraping. *Journal of adhesion science and technology* **22**, 395-402.
[22] King, D.R., Bartlett, M.D., Gilman, C.A., Irschick, D.J. & Crosby, A.J. 2014 Creating gecko-like adhesives for "real world" surfaces. *Adv. Mater.* **26**, 4345-4351.
[23] Lin, H., Lizarraga, L., Bottomley, L.A. & Meredith, J.C. 2015 Effect of water absorption on pollen adhesion. *J. Colloid Interf. Sci.* **442**, 133-139.
[24] Lißner, M., Alabort, E., Erice, B., Cui, H., Blackman, B.R. & Petrinic, N. 2020 On the dynamic response of adhesively bonded structures. *Int. J. Impact Eng.* **138**, 103479.
[25] Ma, Y., Ma, S., Wu, Y., Pei, X., Gorb, S.N., Wang, Z., Liu, W. & Zhou, F. 2018 Remote control over underwater dynamic attachment/detachment and locomotion. *Adv. Mater.* **30**, 1801595.
[26] Haghanifar, S., Lu, P., Kayes, M.I., Tan, S., Kim, K.-J., Gao, T., Ohodnicki, P. & Leu, P.W. 2018 Self-cleaning, high transmission, near unity haze OTS/silica nanostructured glass. *J. Mater. Chem. C* **6**, 9191-9199.
[27] Guo, P., Zheng, Y., Liu, C., Ju, J. & Jiang, L. 2012 Directional shedding-off of water on natural/bio-mimetic taper-ratchet array surfaces. *Soft Matter* **8**, 1770-1775.
[28] Lou, X., Huang, Y., Yang, X., Zhu, H., Heng, L. & Xia, F. 2020 External Stimuli Responsive Liquid-Infused Surfaces Switching between Slippery and Nonslippery States: Fabrications and Applications. *Adv. Funct. Mater.* **30**, 1901130.
[29] Lee, S.G., Kim, H., Choi, H.H., Bong, H., Park, Y.D., Lee, W.H. & Cho, K. 2013 Evaporation-Induced Self-Alignment and Transfer of Semiconductor Nanowires by Wrinkled Elastomeric Templates. *Adv. Mater.* **25**, 2162-2166.
[30] Liu, C., Ding, H., Wu, Z., Gao, B., Fu, F., Shang, L., Gu, Z. & Zhao, Y. 2016 Tunable Structural Color Surfaces with Visually Self-Reporting Wettability. *Adv. Funct. Mater.* **26**, 7937-7942.
[31] Wang, Y., Qian, B., Lai, C., Wang, X., Ma, K., Guo, Y., Zhu, X., Fei, B. & Xin, J.H. 2017 Flexible slippery surface to manipulate droplet coalescence and sliding, and its practicability in wind-resistant water collection. *ACS Appl. Mater. Inter.* **9**, 24428-24432.
[32] Yao, X., Hu, Y., Grinthal, A., Wong, T.-S., Mahadevan, L. & Aizenberg, J. 2013 Adaptive fluid-infused porous films with tunable transparency and wettability. *Nature materials* **12**, 529-534.
[33] Coux, M., Clanet, C. & Quéré, D. 2017 Soft, elastic, water-repellent materials. *Appl. Phys. Lett.* **110**, 251605.
[34] Zhang, P., Liu, H., Meng, J., Yang, G., Liu, X., Wang, S. & Jiang, L. 2014 Grooved organogel surfaces towards anisotropic sliding of water droplets. *Adv. Mater.* **26**, 3131-3135.
[35] Wang, J.N., Liu, Y.Q., Zhang, Y.L., Feng, J., Wang, H., Yu, Y.H. & Sun, H.B. 2018 Wearable superhydrophobic elastomer skin with switchable wettability. *Adv. Funct. Mater.* **28**, 1800625.
[36] Feng, R., Xu, C., Song, F., Wang, F., Wang, X.-L. & Wang, Y.-Z. 2020 A Bioinspired slippery surface with stable lubricant impregnation for efficient water harvesting. *ACS Appl. Mater. Inter.* **12**, 12373-12381.
[37] Li, J., Ueda, E., Paulssen, D. & Levkin, P.A. 2019 Slippery lubricant-infused surfaces: properties and emerging applications. *Adv. Funct. Mater.* **29**, 1802317.
[38] Villegas, M., Zhang, Y., Abu Jarad, N., Soleymani, L. & Didar, T.F. 2019 Liquid-infused surfaces: a review of theory, design, and applications. *ACS Nano* **13**, 8517-8536.
[39] Wong, T.-S., Kang, S.H., Tang, S.K., Smythe, E.J., Hatton, B.D., Grinthal, A. & Aizenberg, J. 2011 Bioinspired self-repairing slippery surfaces with pressure-stable omniphobicity. *Nature* **477**, 443-447.

[40] Su, Y., Cai, S., Wu, T., Li, C., Huang, Z., Zhang, Y., Wu, H., Hu, K., Chen, C. & Li, J. 2019 Smart stretchable janus membranes with tunable collection rate for fog harvesting. *Adv. Mater. Interfaces* **6**, 1901465.
[41] Jiang, S., Hu, Y., Wu, H., Zhang, Y., Zhang, Y., Wang, Y., Zhang, Y., Zhu, W., Li, J. & Wu, D. 2019 Multifunctional janus microplates arrays actuated by magnetic fields for water/light switches and bio-inspired assimilatory coloration. *Adv. Mater.* **31**, 1807507.
[42] Timonen, J.V., Latikka, M., Leibler, L., Ras, R.H. & Ikkala, O. 2013 Switchable static and dynamic self-assembly of magnetic droplets on superhydrophobic surfaces. *Science* **341**, 253-257.
[43] Zhou, Y., Huang, S. & Tian, X. 2020 Magnetoresponsive surfaces for manipulation of nonmagnetic liquids: Design and applications. *Adv. Funct. Mater.* **30**, 1906507.
[44] Tian, D., Zhang, N., Zheng, X., Hou, G., Tian, Y., Du, Y., Jiang, L. & Dou, S.X. 2016 Fast responsive and controllable liquid transport on a magnetic fluid/nanoarray composite interface. *ACS Nano* **10**, 6220-6226.
[45] Li, D., Feng, S., Xing, Y., Deng, S., Zhou, H. & Zheng, Y. 2017 Directional bouncing of droplets on oblique two-tier conical structures. *RSC Adv.* **7**, 35771-35775.
[46] Lin, Y., Hu, Z., Zhang, M., Xu, T., Feng, S., Jiang, L. & Zheng, Y. 2018 Magnetically induced low adhesive direction of nano/micropillar arrays for microdroplet transport. *Advanced Functional Materials* **28**, 1800163.
[47] Wang, W., Timonen, J.V., Carlson, A., Drotlef, D.-M., Zhang, C.T., Kolle, S., Grinthal, A., Wong, T.-S., Hatton, B. & Kang, S.H. 2018 Multifunctional ferrofluid-infused surfaces with reconfigurable multiscale topography. *Nature* **559**, 77-82.
[48] Huang, Y., Stogin, B.B., Sun, N., Wang, J., Yang, S. & Wong, T.S. 2017 A Switchable Cross-Species Liquid Repellent Surface. *Advanced Materials* **29**, 1604641.
[49] Feng, H., Xu, X., Hao, W., Du, Y., Tian, D. & Jiang, L. 2016 Magnetic field actuated manipulation and transfer of oil droplets on a stable underwater superoleophobic surface. *Phys. Chem. Chem. Phys.* **18**, 16202-16207.
[50] Peng, Y., He, Y., Yang, S., Ben, S., Cao, M., Li, K., Liu, K. & Jiang, L. 2015 Magnetically induced fog harvesting via flexible conical arrays. *Adv. Funct. Mater.* **25**, 5967-5971.
[51] Li, D., Huang, J., Han, G. & Guo, Z. 2018 A facile approach to achieve bioinspired PDMS@ Fe 3 O 4 fabric with switchable wettability for liquid transport and water collection. *J. Mater. Chem. A* **6**, 22741-22748.
[52] Liu, M., Wang, S., Wei, Z., Song, Y. & Jiang, L. 2009 Bioinspired design of a superoleophobic and low adhesive water/solid interface. *Adv. Mater.* **21**, 665-669.
[53] Yao, X., Ju, J., Yang, S., Wang, J. & Jiang, L. 2014 Temperature-Driven Switching of Water Adhesion on Organogel Surface. *Advanced Materials* **26**, 1895-1900.
[54] Xie, T. 2011 Recent advances in polymer shape memory. *Polymer* **52**, 4985-5000.
[55] Song, Y., Chen, X., Dabade, V., Shield, T.W. & James, R.D. 2013 Enhanced reversibility and unusual microstructure of a phase-transforming material. *Nature* **502**, 85-88.
[56] Davidson, E.C., Kotikian, A., Li, S., Aizenberg, J. & Lewis, J.A. 2020 3D printable and reconfigurable liquid crystal elastomers with light-induced shape memory via dynamic bond exchange. *Adv. Mater.* **32**, 1905682.
[57] Nonoyama, T., Lee, Y.W., Ota, K., Fujioka, K., Hong, W. & Gong, J.P. 2020 Instant thermal switching from soft hydrogel to rigid plastics inspired by thermophile proteins. *Adv. Mater.* **32**, 1905878.

[58] Li, P., Wang, L., Tang, S., Xing, Y., Zhao, H. & Liu, J. 2020 Shape Control of Lotus Leaf Induced by Surface Submillimeter Texture. *Adv. Mater. Interfaces* **7**, 2000040.
[59] Xie, T. 2010 Tunable polymer multi-shape memory effect. *Nature* **464**, 267-270.
[60] Lin, Y., Hu, Z., Gao, C., Guo, Z., Li, C. & Zheng, Y. 2018 Directional Droplet Spreading Transport Controlled on Tilt-Angle Pillar Arrays. *Adv. Mater. Interfaces* **5**, 1800962.
[61] Cheng, Z., Zhang, D., Lv, T., Lai, H., Zhang, E., Kang, H., Wang, Y., Liu, P., Liu, Y. & Du, Y. 2018 Superhydrophobic shape memory polymer arrays with switchable isotropic/anisotropic wetting. *Adv. Funct. Mater.* **28**, 1705002.
[62] Hu, Z., Zhang, X. & Li, Y. 1995 Synthesis and application of modulated polymer gels. *Science* **269**, 525-527.
[63] Shang, J. & Theato, P. 2018 Smart composite hydrogel with pH-, ionic strength-and temperature-induced actuation. *Soft Matter* **14**, 8401-8407.
[64] Pastorczak, M., Okrasa, L., Yoon, J.A., Kowalewski, T. & Matyjaszewski, K. 2017 Kinetics of the temperature-induced volume phase transition in poly (2-(2-methoxyethoxy) ethyl methacrylate) hydrogels of various topologies. *Polymer* **110**, 25-35.
[65] Li, Y.-Y., Dai, Y., Zhang, X.-Z. & Zhuo, R.-X. 2008 The tuned-morphology studies of the complexes between poly (N-isopropylacrylamide)-b-poly (vinylpyridine) and poly (N-isopropylacrylamide-co-hydroxylethyl methacrylate)-b-poly (vinylphenol). *J. Colloid Interf. Sci.* **328**, 211-215.
[66] Wang, R., Wang, M., Wang, C., Yang, Q., Wang, J. & Jiang, L. 2019 Thermally Driven Interfacial Switch between Adhesion and Antiadhesion on Gas Bubbles in Aqueous Media. *ACS Appl. Mater. Inter.* **11**, 37365-37370.
[67] Hou, Y., Gao, L., Feng, S., Chen, Y., Xue, Y., Jiang, L. & Zheng, Y. 2013 Temperature-triggered directional motion of tiny water droplets on bioinspired fibers in humidity. *Chem. Commun.* **49**, 5253-5255.
[68] Li, C., Yu, C., Hao, D., Wu, L., Dong, Z. & Jiang, L. 2018 Smart Liquid Transport on Dual Biomimetic Surface via Temperature Fluctuation Control. *Advanced Functional Materials* **28**, 1707490.
[69] Leidenfrost, J.G. 1966 On the fixation of water in diverse fire. *International Journal of Heat and Mass Transfer* **9**, 1153-1166.
[70] Zhong, L. & Guo, Z. 2017 Effect of surface topography and wettability on the Leidenfrost effect. *Nanoscale* **9**, 6219-6236.
[71] Graeber, G., Regulagadda, K., Hodel, P., Küttel, C., Landolf, D., Schutzius, T.M. & Poulikakos, D. 2021 Leidenfrost droplet trampolining. *Nature Communications* **12**, 1-7.
[72] Wang, J., Huang, Y., You, K., Yang, X., Song, Y., Zhu, H., Xia, F. & Jiang, L. 2019 Temperature-Driven Precise Control of Biological Droplet's Adhesion on a Slippery Surface. *ACS Appl. Mater. Inter.* **11**, 7591-7599.
[73] Masum, A., Chandrapala, J., Huppertz, T., Adhikari, B. & Zisu, B. 2020 Effect of storage conditions on the physicochemical properties of infant milk formula powders containing different lactose-to-maltodextrin ratios. *Food Chem.* **319**, 126591.
[74] Miguet, J., Pasquet, M., Rouyer, F., Fang, Y. & Rio, E. 2020 Stability of big surface bubbles: impact of evaporation and bubble size. *Soft Matter* **16**, 1082-1090.
[75] Qu, J., Escobar, L., Li, J., Rao, Z. & Xu, B. 2020 Experimental study of evaporation and crystallization of brine droplets under different temperatures and humidity levels. *Int. Commun. Heat Mass* **110**, 104427.

[76] Ma, Y., Ma, S., Yang, W., Yu, B., Pei, X., Zhou, F. & Liu, W. 2019 Sundew-Inspired Simultaneous Actuation and Adhesion/Friction Control for Reversibly Capturing Objects Underwater. *Advanced Materials Technologies* **4**, 1800467.
[77] Liu, H., Zhang, X., Wang, S. & Jiang, L. 2015 Underwater thermoresponsive surface with switchable oil-wettability between superoleophobicity and superoleophilicity. *Small* **11**, 3338-3342.
[78] Chen, L., Liu, M., Lin, L., Zhang, T., Ma, J., Song, Y. & Jiang, L. 2010 Thermal-responsive hydrogel surface: tunable wettability and adhesion to oil at the water/solid interface. *Soft Matter* **6**, 2708-2712.
[79] Heng, L., Li, J., Li, M., Tian, D., Fan, L.Z., Jiang, L. & Tang, B.Z. 2014 Ordered honeycomb structure surface generated by breath figures for liquid reprography. *Adv. Funct. Mater.* **24**, 7241-7248.
[80] Verheijen, H. & Prins, M. 1999 Reversible electrowetting and trapping of charge: model and experiments. *Langmuir* **15**, 6616-6620.
[81] Guo, T., Che, P., Heng, L., Fan, L. & Jiang, L. 2016 Anisotropic Slippery Surfaces: Electric-Driven Smart Control of a Drop's Slide. *Adv. Mater.* **28**, 6999-7007.
[82] Wang, Z., Heng, L. & Jiang, L. 2018 Effect of lubricant viscosity on the self-healing properties and electrically driven sliding of droplets on anisotropic slippery surfaces. *Journal of Materials Chemistry A* **6**, 3414-3421.
[83] Yan, Y., Guo, Z., Zhang, X., He, L., Li, Y., Liu, K., Cai, J., Tian, D. & Jiang, L. 2018 Electrowetting-Induced Stiction Switch of a Microstructured Wire Surface for Unidirectional Droplet and Bubble Motion. *Advanced Functional Materials* **28**, 1800775.
[84] Li, J., Ha, N.S. & van Dam, R.M. 2019 Ionic-surfactant-mediated electro-dewetting for digital microfluidics. *Nature* **572**, 507-510.
[85] Liu, Y., Zhao, L., Lin, J. & Yang, S. 2019 Electrodeposited surfaces with reversibly switching interfacial properties. *Sci. Adv.* **5**, eaax0380.
[86] Oh, I., Keplinger, C., Cui, J., Chen, J., Whitesides, G.M., Aizenberg, J. & Hu, Y. 2018 Dynamically actuated liquid-infused poroelastic film with precise control over droplet dynamics. *Adv. Funct. Mater.* **28**, 1802632.
[87] Wang, J., Sun, L., Zou, M., Gao, W., Liu, C., Shang, L., Gu, Z. & Zhao, Y. 2017 Bioinspired shape-memory graphene film with tunable wettability. *Science advances* **3**, e1700004.
[88] Wang, Q., Xu, B., Hao, Q., Wang, D., Liu, H. & Jiang, L. 2019 In situ reversible underwater superwetting transition by electrochemical atomic alternation. *Nat. Commun.* **10**, 1-8.
[89] Ding, C., Zhu, Y., Liu, M., Feng, L., Wan, M. & Jiang, L. 2012 PANI nanowire film with underwater superoleophobicity and potential-modulated tunable adhesion for no loss oil droplet transport. *Soft Matter* **8**, 9064-9068.
[90] Li, G., Pan, J., Zheng, H., Liu, S. & Tang, J. 2019 Directional motion of dielectric droplets on polymer-coated conductor driven by electric corona discharge. *Appl. Phys. Lett.* **114**, 143701.
[91] Plog, J., Löwe, J.-M., Jiang, Y., Pan, Y. & Yarin, A. 2019 Control of direct written ink droplets using electrowetting. *Langmuir* **35**, 11023-11036.
[92] Liu, X., Ye, Q., Yu, B., Liang, Y., Liu, W. & Zhou, F. 2010 Switching water droplet adhesion using responsive polymer brushes. *Langmuir* **26**, 12377-12382.
[93] Liang, R., Ding, J., Gao, S. & Qin, W. 2017 Mussel-Inspired Surface-Imprinted Sensors for Potentiometric Label-Free Detection of Biological Species. *Angew. Chem. Int. Ed.* **56**, 6833-6837.
[94] Bongiovanni Abel, S., Riberi, K., Rivarola, C.R., Molina, M. & Barbero, C.A. 2019 Synthesis of a smart conductive block copolymer responsive to heat and near infrared light. *Polymers-Basel* **11**, 1744.

[95] Ferreira, G., Goswami, S., Nandy, S., Pereira, L., Martins, R. & Fortunato, E. 2020 Touch-Interactive Flexible Sustainable Energy Harvester and Self-Powered Smart Card. *Adv. Funct. Mater.* **30**, 1908994.
[96] Liu, J., Kim, Y.S., Richardson, C.E., Tom, A., Ramakrishnan, C., Birey, F., Katsumata, T., Chen, S., Wang, C. & Wang, X. 2020 Genetically targeted chemical assembly of functional materials in living cells, tissues, and animals. *Science* **367**, 1372-1376.
[97] Singh, V.K., Kushwaha, C.S. & Shukla, S. 2020 Potentiometric detection of copper ion using chitin grafted polyaniline electrode. *International journal of biological macromolecules* **147**, 250-257.
[98] Xiao, K., Jiang, D., Amal, R. & Wang, D.W. 2018 A 2D Conductive Organic–Inorganic Hybrid with Extraordinary Volumetric Capacitance at Minimal Swelling. *Adv. Mater.* **30**, 1800400.
[99] Ugur, A., Katmis, F., Li, M., Wu, L., Zhu, Y., Varanasi, K.K. & Gleason, K.K. 2015 Low-dimensional conduction mechanisms in highly conductive and transparent conjugated polymers. *Adv. Mater.* **27**, 4604-4610.
[100] Tian, D., He, L., Zhang, N., Zheng, X., Dou, Y., Zhang, X., Guo, Z. & Jiang, L. 2016 Electric field and gradient microstructure for cooperative driving of directional motion of underwater oil droplets. *Adv. Funct. Mater.* **26**, 7986-7992.
[101] Liu, M., Nie, F.-Q., Wei, Z., Song, Y. & Jiang, L. 2010 In situ electrochemical switching of wetting state of oil droplet on conducting polymer films. *Langmuir* **26**, 3993-3997.
[102] Hu, L., Wan, Y., Zhang, Q. & Serpe, M.J. 2020 Harnessing the Power of Stimuli-Responsive Polymers for Actuation. *Adv. Funct. Mater.* **30**, 1903471.
[103] Chen, J., Tao, X., Li, C., Ma, Y., Tao, L., Zheng, D., Zhu, J., Li, H., Li, R. & Yang, Q. 2020 Synthesis of bipyridine-based covalent organic frameworks for visible-light-driven photocatalytic water oxidation. *Appl. Catal. B-Environ.* **262**, 118271.
[104] Sun, R.-D., Nakajima, A., Fujishima, A., Watanabe, T. & Hashimoto, K. 2001 Photoinduced surface wettability conversion of ZnO and TiO2 thin films. *J. Phys. Chem. B* **105**, 1984-1990.
[105] Li, W., Guo, T., Meng, T., Huang, Y., Li, X., Yan, W., Wang, S. & Li, X. 2013 Enhanced reversible wettability conversion of micro-nano hierarchical TiO2/SiO2 composite films under UV irradiation. *Appl. Surf. Sci.* **283**, 12-18.
[106] Zhu, W., Feng, X., Feng, L. & Jiang, L. 2006 UV-Manipulated wettability between superhydrophobicity and superhydrophilicity on a transparent and conductive SnO 2 nanorod film. *Chem. Commun.*, 2753-2755.
[107] Feng, X., Feng, L., Jin, M., Zhai, J., Jiang, L. & Zhu, D. 2004 Reversible super-hydrophobicity to super-hydrophilicity transition of aligned ZnO nanorod films. *J. Am. Chem. Soc.* **126**, 62-63.
[108] Malm, J., Sahramo, E., Karppinen, M. & Ras, R.H. 2010 Photo-controlled wettability switching by conformal coating of nanoscale topographies with ultrathin oxide films. *Chemistry of Materials* **22**, 3349-3352.
[109] Wang, Z., Liu, Y., Guo, P., Heng, L. & Jiang, L. 2018 Photoelectric synergetic responsive slippery surfaces based on tailored anisotropic films generated by interfacial directional freezing. *Advanced Functional Materials* **28**, 1801310.
[110] Han, K., Heng, L., Zhang, Y., Liu, Y. & Jiang, L. 2019 Slippery surface based on photoelectric responsive nanoporous composites with optimal wettability region for droplets' multifunctional manipulation. *Advanced Science* **6**, 1801231.
[111] Li, J., Jing, Z., Yang, Y., Zha, F., Yan, L. & Lei, Z. 2014 Reversible low adhesive to high adhesive superhydrophobicity transition on ZnO nanoparticle surfaces. *Applied surface science* **289**, 1-5.

[112] Liu, K., Cao, M., Fujishima, A. & Jiang, L. 2014 Bio-inspired titanium dioxide materials with special wettability and their applications. *Chemical reviews* **114**, 10044-10094.
[113] Shami, Z. & Holakooei, P. 2020 Durable light-driven three-dimensional smart switchable superwetting nanotextile as a green scaled-up oil–water separation technology. *ACS omega* **5**, 4962-4972.
[114] Velayi, E. & Norouzbeigi, R. 2018 Annealing temperature dependent reversible wettability switching of micro/nano structured ZnO superhydrophobic surfaces. *Applied Surface Science* **441**, 156-164.
[115] Wang, H. & Guo, Z. 2014 Design of underwater superoleophobic TiO2 coatings with additional photo-induced self-cleaning properties by one-step route bio-inspired from fish scales. *Applied Physics Letters* **104**, 183703.
[116] Yong, J., Chen, F., Yang, Q., Farooq, U. & Hou, X. 2015 Photoinduced switchable underwater superoleophobicity–superoleophilicity on laser modified titanium surfaces. *Journal of Materials Chemistry A* **3**, 10703-10709.
[117] Zhu, X., Zhang, Z., Men, X., Yang, J. & Xu, X. 2010 Fabrication of an intelligent superhydrophobic surface based on ZnO nanorod arrays with switchable adhesion property. *Applied Surface Science* **256**, 7619-7622.
[118] Gao, F., Yao, Y., Wang, W., Wang, X., Li, L., Zhuang, Q. & Lin, S. 2018 Light-driven transformation of bio-inspired superhydrophobic structure via reconfigurable PAzoMA microarrays: From lotus leaf to rice leaf. *Macromolecules* **51**, 2742-2749.
[119] Gao, C., Wang, L., Lin, Y., Li, J., Liu, Y., Li, X., Feng, S. & Zheng, Y. 2018 Droplets manipulated on photothermal organogel surfaces. *Advanced Functional Materials* **28**, 1803072.
[120] Ennaceri, H., Wang, L., Erfurt, D., Riedel, W., Mangalgiri, G., Khaldoun, A., El Kenz, A., Benyoussef, A. & Ennaoui, A. 2016 Water-resistant surfaces using zinc oxide structured nanorod arrays with switchable wetting property. *Surface and Coatings Technology* **299**, 169-176.
[121] Liu, Y., Lin, Z., Lin, W., Moon, K.S. & Wong, C. 2012 Reversible superhydrophobic–superhydrophilic transition of ZnO nanorod/epoxy composite films. *ACS applied materials & interfaces* **4**, 3959-3964.
[122] Djurišić, A.B., Chen, X., Leung, Y.H. & Ng, A.M.C. 2012 ZnO nanostructures: growth, properties and applications. *J. Mater. Chem.* **22**, 6526-6535.
[123] Xu, L., Hu, Y.-L., Pelligra, C., Chen, C.-H., Jin, L., Huang, H., Sithambaram, S., Aindow, M., Joesten, R. & Suib, S.L. 2009 ZnO with different morphologies synthesized by solvothermal methods for enhanced photocatalytic activity. *Chem. Mater.* **21**, 2875-2885.
[124] Zhang, Y.S. & Khademhosseini, A. 2017 Advances in engineering hydrogels. *Science* **356**.
[125] Wei, J. & Yu, Y. 2012 Photodeformable polymer gels and crosslinked liquid-crystalline polymers. *Soft Matter* **8**, 8050-8059.
[126] Wang, E., Desai, M.S. & Lee, S.-W. 2013 Light-controlled graphene-elastin composite hydrogel actuators. *Nano Lett.* **13**, 2826-2830.
[127] Bijlard, A.C., Wald, S., Crespy, D., Taden, A., Wurm, F.R. & Landfester, K. 2017 Functional Colloidal Stabilization. *Adv. Mater. Interfaces* **4**, 1600443.
[128] Ding, L., Li, Y., Cang, H., Li, J., Wang, C. & Song, W. 2020 Controlled synthesis of azobenzene-containing block copolymers both in the main-and side-chain from SET-LRP polymers via ADMET polymerization. *Polymer* **190**, 122229.

[129] Mohan, A., Sasikumar, D., Bhat, V. & Hariharan, M. 2020 Metastable Chiral Azobenzenes Stabilized in a Double Racemate. *Angew. Chem. Int. Ed.* **59**, 3201-3208.
[130] Sutton, A., Shirman, T., Timonen, J.V., England, G.T., Kim, P., Kolle, M., Ferrante, T., Zarzar, L.D., Strong, E. & Aizenberg, J. 2017 Photothermally triggered actuation of hybrid materials as a new platform for in vitro cell manipulation. *Nat. Commun.* **8**, 1-13.
[131] Zhang, Q.M., Li, X., Islam, M.R., Wei, M. & Serpe, M.J. 2014 Light switchable optical materials from azobenzene crosslinked poly (N-isopropylacrylamide)-based microgels. *J. Mater. Chem. C* **2**, 6961-6965.
[132] Nie, J., Liu, X., Yan, Y. & Zhang, H. 2017 Supramolecular hydrogen-bonded photodriven actuators based on an azobenzene-containing main-chain liquid crystalline poly (ester-amide). *J. Mater. Chem. C* **5**, 10391-10398.
[133] Lv, J.-a., Liu, Y., Wei, J., Chen, E., Qin, L. & Yu, Y. 2016 Photocontrol of fluid slugs in liquid crystal polymer microactuators. *Nature* **537**, 179-184.
[134] Cheng, Z., Ma, S., Zhang, Y., Huang, S., Chen, Y. & Yu, H. 2017 Photomechanical motion of liquid-crystalline fibers bending away from a light source. *Macromolecules* **50**, 8317-8324.
[135] Li, Y., He, Y., Tong, X. & Wang, X. 2005 Photoinduced deformation of amphiphilic azo polymer colloidal spheres. *J. Am. Chem. Soc.* **127**, 2402-2403.
[136] Bai, J., Shi, Z., Yin, J., Tian, M. & Qu, R. 2018 Shape reconfiguration of a biomimetic elastic membrane with a switchable Janus structure. *Adv. Funct. Mater.* **28**, 1800939.
[137] Ikejiri, S., Takashima, Y., Osaki, M., Yamaguchi, H. & Harada, A. 2018 Solvent-free photoresponsive artificial muscles rapidly driven by molecular machines. *J. Am. Chem. Soc.* **140**, 17308-17315.
[138] Ge, F., Lu, X., Xiang, J., Tong, X. & Zhao, Y. 2017 An optical actuator based on gold-nanoparticle-containing temperature-memory semicrystalline polymers. *Angew. Chem. Int. Ed.* **129**, 6222-6226.
[139] Xue, C.-H., Li, Y.-R., Hou, J.-L., Zhang, L., Ma, J.-Z. & Jia, S.-T. 2015 Self-roughened superhydrophobic coatings for continuous oil–water separation. *J. Mater. Chem. A* **3**, 10248-10253.
[140] Wang, R., Hashimoto, K., Fujishima, A., Chikuni, M., Kojima, E., Kitamura, A., Shimohigoshi, M. & Watanabe, T. 1997 Light-induced amphiphilic surfaces. *Nature* **388**, 431-432.
[141] Elazab, A., Serret, M.D. & Araus, J.L. 2016 Interactive effect of water and nitrogen regimes on plant growth, root traits and water status of old and modern durum wheat genotypes. *Planta* **244**, 125-144.
[142] Schwerbrock, R. & Leuschner, C. 2016 Air humidity as key determinant of morphogenesis and productivity of the rare temperate woodland fern Polystichum braunii. *Plant Biology* **18**, 649-657.
[143] Prodanovic, V., Wang, A. & Deletic, A. 2019 Assessing water retention and correlation to climate conditions of five plant species in greywater treating green walls. *Water Res.* **167**, 115092.
[144] Qu, R., Zhang, W., Li, X., Liu, Y., Wei, Y., Feng, L. & Jiang, L. 2020 Peanut Leaf-Inspired Hybrid Metal–Organic Framework with Humidity-Responsive Wettability: toward Controllable Separation of Diverse Emulsions. *ACS Appl. Mater. Inter.* **12**, 6309-6318.
[145] Li, C., Liu, Y., Gao, C., Li, X., Xing, Y. & Zheng, Y. 2019 Fog harvesting of a bioinspired nanocone-decorated 3D fiber network. *ACS Appl. Mater. Inter.* **11**, 4507-4513.
[146] Jiang, W., Upadhyaya, P., Zhang, W., Yu, G., Jungfleisch, M.B., Fradin, F.Y., Pearson, J.E., Tserkovnyak, Y., Wang, K.L. & Heinonen, O. 2015 Blowing magnetic skyrmion bubbles. *Science* **349**, 283-286.

[147] Li, P., Han, Y., Zhou, X., Fan, Z., Xu, S., Cao, K., Meng, F., Gao, L., Song, J. & Zhang, H. 2020 Thermal effect and Rayleigh instability of ultrathin 4H hexagonal gold nanoribbons. *Matter* **2**, 658-665.
[148] Pham, C.-T., Perrard, S. & Le Doudic, G. 2020 Surface waves along liquid cylinders. Part 1. Stabilising effect of gravity on the Plateau–Rayleigh instability. *J. Fluid Mech.* **891**.
[149] Cheng, Z., Lai, H., Du, Y., Fu, K., Hou, R., Li, C., Zhang, N. & Sun, K. 2014 pH-induced reversible wetting transition between the underwater superoleophilicity and superoleophobicity. *ACS Appl. Mater. Inter.* **6**, 636-641.
[150] Huang, X., Mutlu, H. & Theato, P. 2020 A bioinspired hierarchical underwater superoleophobic surface with reversible pH response. *Advanced Materials Interfaces* **7**, 2000101.
[151] Zhang, L., Zhang, Z. & Wang, P. 2012 Smart surfaces with switchable superoleophilicity and superoleophobicity in aqueous media: toward controllable oil/water separation. *NPG Asia Mater.* **4**, e8-e8.
[152] Cheng, Q., Li, M., Yang, F., Liu, M., Li, L., Wang, S. & Jiang, L. 2012 An underwater pH-responsive superoleophobic surface with reversibly switchable oil-adhesion. *Soft Matter* **8**, 6740-6743.
[153] Andreozzi, A., Iasiello, M. & Netti, P. 2020 Effects of pulsating heat source on interstitial fluid transport in tumour tissues. *Journal of the Royal Society Interface* **17**, 20200612.
[154] Arzani, A. 2018 Accounting for residence-time in blood rheology models: do we really need non-Newtonian blood flow modelling in large arteries? *Journal of The Royal Society Interface* **15**, 20180486.
[155] Hsu, C.-P., Mandal, J., Ramakrishna, S.N., Spencer, N.D. & Isa, L. 2021 Exploring the roles of roughness, friction and adhesion in discontinuous shear thickening by means of thermo-responsive particles. *Nature communications* **12**, 1-10.
[156] Chen, Y., Meng, J., Gu, Z., Wan, X., Jiang, L. & Wang, S. 2020 Bioinspired multiscale wet adhesive surfaces: structures and controlled adhesion. *Advanced Functional Materials* **30**, 1905287.
[157] Dai, B., Li, K., Shi, L., Wan, X., Liu, X., Zhang, F., Jiang, L. & Wang, S. 2019 Bioinspired janus textile with conical micropores for human body moisture and thermal management. *Advanced Materials* **31**, 1904113.

Authors' Biography

Chang Li is a PhD researcher of AVIC Centre for Structural Design and Manufacture at Imperial College London. He awarded his postgraduate degree from Beihang University in 2019, under the supervision of Prof. Yongmei Zheng. He focuses on surface adhesion property & water behaviour on bioinspired nanomaterials, as well as surface pre-treatment & characterisation of composites for adhesive bonding.

Ming Li is a member of the President Scholar Group (2019-2023) currently, and pursuing his Ph.D. degree under the supervision of Prof. Eduardo Saiz at the Center of Advanced Structural Ceramics, Department of Materials, Imperial College London, the UK. His research interest focuses on the design and fabrication of bio-inspired interfacial materials with controllable adhesion and wettability, as well as the construction of smart soft materials, e.g. responsive and bioinspired hydrogels.

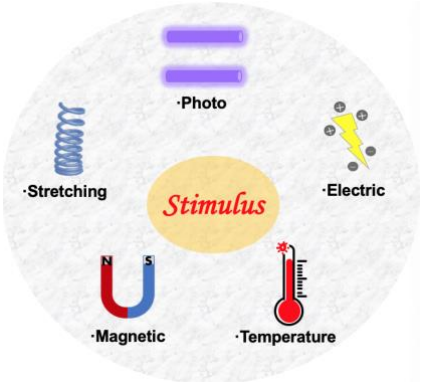

Table of Contents Graphic